CODEN:LUTEDX/(TEIE-5324)/1-49/(2013)

Industrial Electrical Engineering and Automation

Dynamic Line Rating

Thermal Line Model and Control

Martin Andersson Ljus

Division of Industrial Electrical Engineering and Automation
Faculty of Engineering, Lund University

Abstract

In times of increased environmental awareness, there exists a desire to not only build new environmentally friendly and renewable power generating units, but also to increase the efficiency of all existing technology. Wind power is such a renewable and environmentally friendly technology. Wind turbines and wind power have made giant leaps in the world in the past years, with an almost exponential growth in production and number of units. This increased utilization puts a lot of stress on the already existing grids, which were oftentimes built without this power increase in mind. To further add to these problems, wind power particularly is something that is not always readily available, neither is it stored.

Dynamic line rating is a way of optimizing the power throughput through the distribution and transmission lines, by not only looking at the current through them as a way to determine its rating, but also by measuring how the weather affects the thermal system. In reality, several factors decide the line rating, which is how much current a line can carry. These weather impacting parameters include; wind speed, wind direction, solar irradiation and ambient temperature, not only the current through the conductor. Normally, the rating of the line is decided conservatively with a fixed value for the maximum current so as to make sure the surface temperature and resulting sag is always within acceptable boundaries. With these additional parameters however, a higher line rating can often be used. Considering the cooling effect of the wind means dynamic line rating is ideal for wind power, since in that case, the wind both produces power while allowing for a higher power throughput on the line. By continuously measuring all of these parameters, one can more effectively determine the rating of a line and the available amount of additional power it can carry, while still meeting regulations.

This thesis explores dynamic line rating in connection with an *E.ON* offshore wind farm project at Kårehamn near Öland in Sweden. This is done by first building a *Simulink* computer model for the continuous determination of the conductor surface temperature – and based on this implementing an algorithm for controlling the output of *Kårehamn* wind farm. Rather than calculating the *ampacity*, the line rating, which is often done, this model will focus on explicitly controlling the temperature – since it is the temperature requirements that must be met in order to meet regulations regarding the line sag, the height of the lines above ground.

A model and a control method were produced, that successfully controlled the surface temperature of the most critical conductor by sending a reference value to control the output of the wind farm. By building thermal models with input parameters such as current (converted from the power value), wind speed, wind direction and ambient temperatures, the surface temperature could be accurately calculated. The control algorithm developed in this work is compared to and found superior to an existing prototype solution used by E.ON. This thesis also successfully incorporated error handling and ways of controlling additional power generating units on the grid.

Table of Contents

Chapter 1. Introduction

This chapter aims at giving a background to the work conducted in this thesis, so it is understood what is done and why. The chapter also establishes the aims of the thesis and limitations of the work.

1.1 Background

Renewable energy is on the rise in Sweden and in the world, with wind power amongst the most expansive risers nationally, with an increase of 74 % in wind power production between 2010 and 2011 [1]. The Swedish government has, in accordance with EU regulations, set environmental targets which amongst others include that 50 % of total energy usage shall come from renewable energy [2].

To meet these targets as well as a possible future increase in energy demand, the distribution network is possibly changing from passive to active with an increasing amount of Distributed Generation such as wind farms being connected to the network. Wind farms tend to be built where there is most wind, wherever it may be. These farms are often located on the edges of the distributions systems, where it may be most convenient to connect them to a local grid, one often not rated to carry the extra loading [3]. There is a desire to increase the power transferred by transmission and distribution lines, though that is not always feasible with existing lines. One solution would be to simply build new lines; overhead conductors or underground cables, though this is expensive.

Dynamic line rating is the continuous measurement of conductor conditions to allow for maximum power throughput. It is the sag of a line section that will determine the maximum permissible temperature of the conductor. Sag of an overhead line is the difference in height between the highest and lowest point of a line section, i.e. between two poles. When the temperature of an overhead line increases, annealing of the metal causes the line section to change in length which changes the sag. The temperature of a conductor depends on the load current, as well as other parameters acting on the conductor, such as ambient temperature, wind speed, wind direction and solar radiation. In the past, default and often relatively conservative values have been set to make sure the temperatures of the conductors are within the desired limits at all times. That means that the lines for the most part would be limited well below their capacity. To actively measure the lines rating, instead of using default conservative values, means the power throughput can be increased most of the time. This is ideal for wind power, because having strong winds allows for higher power output from the generation site, but also allows for more power on the grid, due to the cooling effect of the wind on the conductor.

E.ON wind is building a new offshore wind farm, Kårehamn, east of Föra on Öland, consisting of 16 3 MW wind turbines with a maximal output of 48 MW. The 50 kV-grid on Öland can currently only handle about 20 MW of that power without modifications [4]. As a result, the grid would get overloaded by the new wind farm at certain times, such as when the ambient temperature is high or the local load is at a minimum. This means that the temperature and resulting sag in the line will reach unacceptable levels. Dynamic line rating would allow the lines to carry the maximum amount of power at any given time, minimizing grid curtailment; which is used when more wind power is available than is allowed on the grid.

To accomplish this, E.ON has installed measurement equipment on the lines at three different locations on the grid; at Köping, Högsrum and Linsänkan. The equipment at Köping and Linsänkan will measure the current through the conductors, while the equipment in Högsrum directly measures the surface temperature.

1.2 Aims

The aim of this master thesis is to develop a method for controlling the output of the wind farm Kårehamn, a control algorithm, to make sure that the impact of the wind farm on the local grid never causes the conductor surface temperatures to exceed 50 °C. This will be done by building a model in Simulink, with a thermal model as well as a PID regulator. The regulator will control the surface temperature of the conductor. In the real world application, physical connections will send a power reference value generated by the model to the wind farm.

By measuring the current and temperature of the overhead lines at the three different locations, with each site measuring the two different conductors, the output should be controlled so that the temperature requirements for the conductors are always met. It is furthermore the aim of this thesis to produce methods for handling errors in the system, and to find a way to deal with additional power acting on the grid. These secondary objectives include:

- To develop a method for controlling additional generation units connected to the grid. The additional power, in this case, is one solar park and a wind turbine. Their needs are secondary to Kårehamn, and are thus not allowed to compromise the output from the wind farm. It is desirable to be able to send a control signal, one which will tell them if they are allowed to be connected to the grid or not. This will happen when the conductor surface temperature at one or several of the monitored line sections surpasses 50 °C, as these should always turn off before Kårehamn itself lowers its output.
- To develop a method where preset values are sent as reference values to the wind turbines in case the system is unresponsive and surface temperature gets too high yet not critical.
- To develop an emergency shutdown procedure for Kårehamn, should the surface temperature surpass a preset critical value during a period of time without it reacting to a change in the reference signal being sent.
- To build and test an alternative model which incrementally controls the output of Kårehamn and compare it with the model developed in this thesis
- To investigate if the control system can be tested this early on when just a part of the wind farm is completed.

1.3 Limitations

Since time is limited, focus will primarily be on the thermal model itself and control of the temperature. The secondary aims will be met if there is additional time.

This thesis will be limited to computer models, and thus no concern will be given to the physical implementation. Furthermore, the model will use the temperature to control, and not the current.

Chapter 2. Theory

This chapter introduces the theory behind and regarding the heat balance in an overhead conductor, the physics and equations of them. It also explains data specific to Öland as well as ampacity and current conversion equations.

2.1 Overhead Lines

There are several different types of conductors on Öland, of which only two are relevant for further studies in this thesis; the *159 Al59* and *329 Al59* conductors. That is because only these conductor types are used on the line sections where the measuring stations are located. For detailed information regarding each conductor, please refer to Appendix A.

2.2 Heat balance in an overhead line

The sections herein about the thermal balance on the overhead conductors and its different parameters closely follow those in the CIGRE technical brochure 207, *Thermal Behaviour of Overhead Conductors* [5], unless stated otherwise. There is another commonly used standard for these calculations, namely the *IEEE 738* [6]. Comparisons made between these two standards, show slight differences in ampacity, ranging from 1% to 8.5% [3]. Given that small difference, as well as the fact the CIGRE technical brochure was initially available, that standard was used.

The relationship between the current and temperature in the lines is shown below. It applies for the unsteady state, when the temperature of the conductor is not in thermal equilibrium.

$$\mathrm{m} * \mathrm{c} * \frac{\mathrm{dT}_{av}}{\mathrm{dt}} = \mathrm{P_J} + \mathrm{P_M} + \mathrm{P_i} + \mathrm{P_S} - \mathrm{P_C} - \mathrm{P_R} - \mathrm{P_W}$$

Where:

m = Conductor mass density per unit length (kg/m)
c = Conductor specific heat capacity (J/(kg*K))
T_{av} = Conductor average temperature (°C)
P_J = Current heating per unit length (W/m)
P_M = Magnetic heating per unit length (W/m)
P_i = Corona heating per unit length (W/m)
P_S = Solar heating per unit length (W/m)
P_C = Convective cooling per unit length (W/m)
P_R = Radiative cooling per unit length (W/m)
P_W = Evaporative cooling per unit length (W/m)

Some of these parameters are commonly neglected, such as P_i and P_W.

"P_i and P_W are commonly neglected. For example, for the Lynx conductor, P_M can be neglected because the two layers of Aluminum strand spiral in opposite directions around the steel core, and the magnetic fields largely cancel out. P_i, P_W and P_M are not considered in the P341 DLR calculations." [3]

P_i and P_W will be excluded here as well. The magnetic heating P_M is included in the formula for calculating the current heating P_J. The resulting differential equation is then:

$$\mathrm{m} * \mathrm{c} * \frac{\mathrm{dT}_{av}}{\mathrm{dt}} = \mathrm{P_J} + \mathrm{P_S} - \mathrm{P_C} - \mathrm{P_R}$$

The calculations of the individual terms on the right-hand side of above equation are given below. According to [5], it is generally sufficient to assume that the average temperature of the conductor is equal to its surface temperature T_s, that is; $T_{av}=T_s$. This will be assumed here as well, since the surface temperature is what will be measured in the real case on Öland.

2.2.1 Current heating

Current heating is the heating of the conductor due to the effects of load current and includes both the joule heating as well as magnetic heating. The heat gain is given by:

$$P_J = k_j * I_{dc}^2 * R_{dc} * \left(1 + \alpha * (T_s - 20)\right)$$

Where:

$k_j = R_{ac}/ R_{dc}$ = Factor which takes into account the magnetic heating (unitless)
I_{dc} = Effective current (A)
R_{dc} = Dc resistance (Ω/m), at 20 °C
α = Temperature coefficient of resistance per degree Kelvin (1/K)
T_s = Conductor surface temperature (°C)

2.2.2 Solar heating

Solar heating is the heating of the conductor as a consequence of incoming solar irradiation. The effect of solar heating will not be measured on site, which means that it is not something that will be used in calculations in the real case. However, it is the aim of this thesis to test two cases in the simulations; a case of no solar heating as well as a simplified case of solar heating, to investigate the effects of the solar heating. The simplified equation for calculating the solar heating gain is given below.

$$P_S = \alpha_s * S * D$$

Where:

α_S = Absorptivity of conductor surface (unitless)
S = global solar radiation (W/m^2)
D = external diameter of conductor (m)

2.2.3 Convective cooling

The heat loss due to convective cooling is a major factor in the thermal heat balance. Overhead conductors heat the surrounding air, and as the air heats up, its density decreases, causing it to rise. There are several cases of convective heat loss, depending on wind speed and angle. Forced convection, with wind speeds above zero, causes the heated air to be forcefully carried away, whilst natural convection, with no wind, causes the heated air to naturally rise. There is also a corrective convective cooling, which deals with the cooling at low wind speeds.

For higher wind speeds (i.e. ≥0.5 m/s), the forced convective formula will be used. For lower wind speeds (i.e. <0.5 m/s), the values for the natural, the corrected as well as the forced convective with an assumed angle of 45 ° will be computed, and the largest of them be used.

The convective heat loss is given by:

$$P_C = \pi * \lambda_f * (T_s - T_a) * Nu$$

Nu is the Nusselt number, and it is the one that changes depending on which kind of convection is in effect. The equations for convective cooling below are all taken from the *MiCOM P341 Application Guide* [3], though rewriting the equations in [5] would give the same equations.

For forced convection, the heat loss is given by:

$$P_{C\_forced} = \pi * \lambda_f * (T_s - T_a) * B_1 * \left(\rho_r * V * \frac{D}{v}\right)^n * (A_1 + B_2 * (\sin\delta))^{m_1}$$

For natural convection, the heat loss is given by:

$$P_{C\_natural} = \pi * \lambda_f * (T_s - T_a) * A_2 * \left(D^3 * (T_s - T_a) * \frac{g}{v^2 * (T_f + 273.15)} * Pr\right)^{m_2}$$

The corrected convective heat loss is given by:

$$P_{C\_corrected} = \pi * \lambda_f * (T_s - T_a) * 0{,}55 * B_1 * \left(\rho_r * V * \frac{D}{v}\right)^n$$

Where:

T_a = Ambient temperature (°C)
T_f = Film temperature at surface of conductor = $0{,}5 * (T_a + T_s)$ (°C)
λ_f = Thermal conductivity of air = $2{,}42 * 10^{-2} + 7{,}2 * 10^{-5} * T_f$ (W/(m * K))
g = Gravitational acceleration, constant = 9,82 m/s^2
Pr = Prandtl number = $0{,}715 - 2{,}5 * 10^{-4} * T_f$ (unitless)
ρ_r = Relative air density = $e^{-1{,}16*10^{-4}*y}$, where y is the height above the sea level (unitless)
V = Wind velocity (m/s)
v = Kinematic viscosity = $1{,}32 * 10^{-5} + 9{,}5 * 10^{-8} * T_f$ (m^2/s)
δ = Effective angle between wind and conductor line (°)
D = Overall diameter of the conductor (m)

A_1, A_2, B_1, B_2, m_1 and m_2 are the values determined by the intermediate calculated parameters.

$A_1 = 0{,}42, B_2 = 0{,}68$ and $m_1 = 1{,}08$ for $0° < \delta < 24°$
$A_1 = 0{,}42, B_2 = 0{,}58$ and $m_1 = 0{,}90$ for $24° < \delta < 90°$

$A_2 = 0{,}850, m_2 = 0{,}188$ for $D^3 * (T_s - T_a) * \frac{g}{v^2*(T_f+273.15)} * Pr < 10^4$
$A_2 = 0{,}480, m_2 = 0{,}250$ for $D^3 * (T_s - T_a) * \frac{g}{v^2*(T_f+273.15)} * Pr > 10^4$

$B_1 = 0{,}641, n = 0{,}471$ for $\rho_r * V * \frac{D}{v} \leq 2{,}65 * 10^3$
$B_1 = 0{,}178, n = 0{,}633$ for $\rho_r * V * \frac{D}{v} > 2{,}65 * 10^3$ and $R_f \leq 0{,}05$
$B_1 = 0{,}048, n = 0{,}800$ for $\rho_r * V * \frac{D}{v} > 2{,}65 * 10^3$ and $R_f > 0{,}05$

R_f = Roughness of conductor surface = $\frac{d}{2*(D-d)}$ (unitless), where d is the outer layer wire diameter

2.2.4 Radiative cooling

Radiative heat loss in a conductor is the process by which it loses heat due to thermal radiation. The equation for the radiative cooling is given by:

$$P_R = \pi * D * \varepsilon * \sigma_B * ((T_s + 273.15)^4 - (T_a + 273.15)^4)$$

Where:

$\varepsilon =$ Emissivity (unitless)
$\sigma_B =$ Stefan $-$ Boltzmann constant $= 5{,}67 * 10^{-8}$ $(W/(m^2 * K^4))$
$D =$ Overall conductor diameter (m)

2.3 Time-dependent heating

The thermal time constant τ_h is the time interval for the temperature rise of the conductor, to that of 63.2 % of its final steady state value when subjected to a step change in e.g. current.

$$\tau_h = m * c * \frac{\theta_m}{I^2 * R_{ac} + P_s}$$

The solution to the equation for an increase in current is given by:

$$t_{12} = -\tau_h * \left(\beta * (\theta - \theta_1) + (1 + \beta * \theta_m) * \ln\left(\frac{\theta_m - \theta}{\theta_m - \theta_1}\right)\right)$$

However, since β – which is the temperature coefficient of specific heat capacity – is so small (refer to appendix A), it can and will be neglected here [5], resulting in the simplified equation below:

$$t_{12} = -\tau_h * \ln\left(\frac{\theta_m - \theta}{\theta_m - \theta_1}\right)$$

Where:

θ = average temperature rise of conductor
θ_1 = initial average temperature rise of conductor at time t_1
θ_m = asymptotic average temperature rise of conductor

The behavior of the time-dependent heating can be seen below in Figure 2-1.

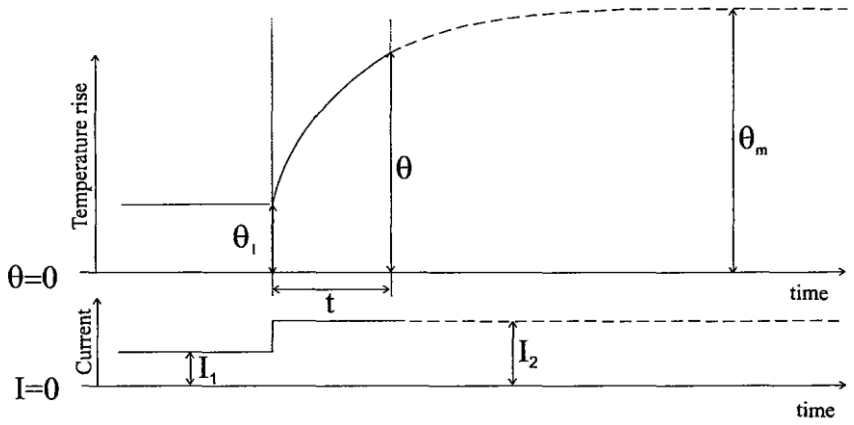

Figure 2-1. [5] Temperature behaviour of an overhead conductor after an increase in current.

2.4 Time-dependent cooling

The thermal time constant here is given by:

$$\tau_c = \frac{m * c * \theta_{m1}}{P_1}$$

The solution to the heat balance equation for a step decrease in current, and with neglected β is given by:

$$t_{12} = -\tau_c * \ln\left(\frac{P_1 * \frac{\theta_2}{\theta_{m1}} - P_2}{P_1 * \frac{\theta_1}{\theta_{m1}} - P_2}\right)$$

Where:

$P_1 = I_1^2 * R_{ac} * (1 + \alpha * \theta_{m1}) + P_s - \alpha * I_1^2 * R_{ac} * \theta_{m1}$
$P_2 = I_1^2 * R_{ac} + P_s$

The behavior of time-dependent cooling can be seen in Figure 2-2 below.

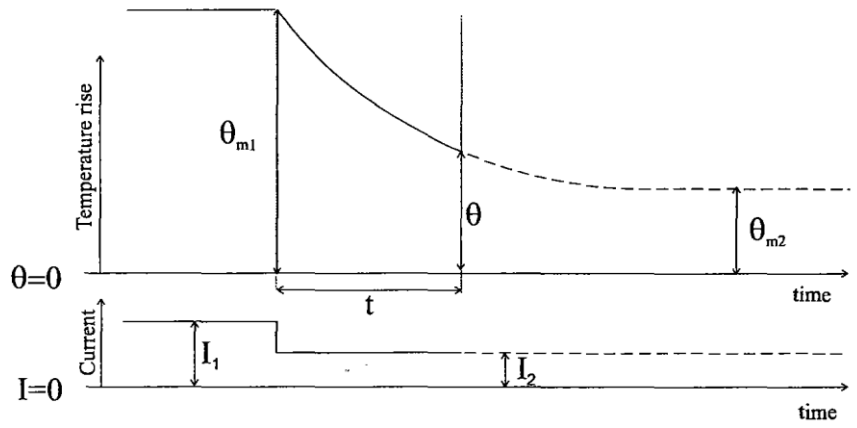

Figure 2-2. [5] Temperature behaviour of an overhead conductor after a decrease in current.

2.5 Ampacity

Ampacity, or the thermal rating of the line, is the maximum current a conductor can carry without exceeding its sag temperature. The sag temperature is the temperature at which the legislated height of the conductor above ground is met.

The ampacity can be measured either directly, or indirectly by measuring ambient weather conditions and then solving equations. The ampacity equation is given below.

$$I_{dc} = \sqrt{\frac{P_C + P_R - P_S}{R_{dc} * \left(1 + \alpha * (T_s - 20)\right)}}$$

The ampacity in dc can then be converted if needed according to the equations in section 2.6.

2.6 Current conversion

It is vital that models for converting between alternating and direct current be implemented, since the thermal model, or current heating model, requires direct current as an input. Meanwhile, the real world application – where Kårehamn feeds the grid on Öland – functions with alternating current. Below are equations regarding current conversion, according to *IEC 60287* [7].

$$R_{dc} = \mathrm{R}_{20} * \left(1 + \alpha * (\mathrm{T} - 20)\right)$$

Where:

R_{dc} = Conductor resistance at temperature T (Ω)
R_{20} = Conductor resistance at 20 °C (Ω)
T = Operating temperature of the conductor (°C)
α = Temperature coefficient of resistance per degree Kelvin (1/K)

$$R_{ac} = \mathrm{R}_{dc} * \left(1 + y_s + y_p\right)$$

Where:

y_s = Skin effect factor
y_p = Proximity effect factor (0 in case of overhead lines)

2.6.1 Skin effect

As the frequency of the current increases, the flow of electricity tends to become more concentrated around the outside of a conductor. At very high frequencies, hollow conductors are often used primarily for this reason. At power frequencies (typically 50 or 60 Hz), while less pronounced the change in resistance due to skin effect is still noticeable. The skin effect factor is given by:

$$y_s = \frac{x_s^4}{192 + 0.8 * x_s^4}$$

Where:

$$x_s = \sqrt{\frac{8 * \pi * f}{R_{dc}} * 10^{-7} * k_s}$$

f = Supply frequency (Hz)
k_s = Skin effect coefficient (=1 for bare conductors)

It is known [5], that:

$$I_{ac}^2 R_{ac} = I_{dc}^2 R_{dc}$$

This yields the following equations:

$$I_{ac} = I_{dc}\sqrt{R_{dc}/R_{ac}}$$

$$I_{ac} = I_{dc}/\sqrt{1 + y_s}$$

When testing the above equations for current conversion, they produced different results, when they should give the same answer. That might be related to the numbers given by E.ON for the resistances, and that the dc resistance given was not specified for any specific temperature, while the ac resistance was specified for 50 °C. The model used the first equation above for the current conversion calculations, since both values for resistances were given.

2.7 Öland, location-specific values

Surface temperature of the conductors will be calculated at three different locations on Öland as mentioned before. Each location will measure both lines, thus giving a total of six different values for the temperature.

Köping and Linsänkan will both have Alstom protective relays and weather stations installed, while Högsrum only have Power Donuts installed. The Alstom relays measure the line current, which means that the temperature will have to be calculated using the current input, as well as weather parameters collected from the weather stations. The power donuts however, measure the surface temperatures directly, meaning it will be readily available to use in the model.

The general theory with all its equations that are going to be used in the thesis, was shown earlier in the chapter. For the specific case on Öland, several additional parameters were needed. Cable specific numbers were provided by E.ON and can be found in Appendix A. In order to calculate the effect of the solar heating, both the global irradiation and the absorptivity of aluminum were needed. Looking at a solar heating map, the worst case scenario for Öland in terms of irradiation was found to be 560 W/m^2 [8], which was the average value at noon for a hot day in June, calculated on a horizontal plane in Öland, near Linsänkan. The value of the absorptivity for aluminum varies widely, as does the emissivity. The emissivity is needed in order to calculate the radiative cooling. Values for these were chosen to be 0.5 and 0.07 respectively (which was the number for rough aluminum) [9], [10]. According to *Thermal Behaviour of Overhead Conductors* a value of 0.5 can be chosen for most purposes, which is in line with what was found on the webpage. The values E.ON themselves use are 0.7 for both absorptivity and emissivity [11].

A number for the relative air density, which is related to the height above sea level, is needed to calculate the convective cooling gains. The height above sea level on Öland was found to be between 5-55 m, with an average of about 35 m [12]. The conductors, in turn, are at a height of about 7 m above ground. So, y = 35 + 7 m = 42 m.

Lastly and also needed to calculate convective cooling, is the roughness of the conductor surface. As can be seen in Appendix A, the conductors are made up of several smaller aluminum strands. The total diameter of the 157 al59 and 329 al59 cables are 16.3 mm and 23.6 mm respectively. The outer layer wire diameter, d, is 3.26 mm. So, the value for R_f is:

$$R_{f\_157al59} = \frac{d}{2*(D-d)} = \frac{3.26}{2*(16.3-3.26)} = 0.125$$

$$R_{f\_329al59} = \frac{d}{2*(D-d)} = \frac{3.26}{2*(23.6-3.26)} = 0.080$$

The value for both cables is larger than 0.05. This is critical in deciding which values are being used in the convective cooling equations, as seen earlier.

Chapter 3. Thermal model

To be able to simulate, test for different values, and eventually realize a control method, a Simulink model for the thermal heat balance had to be made. The thermal system created is shown in Figure 3-1.

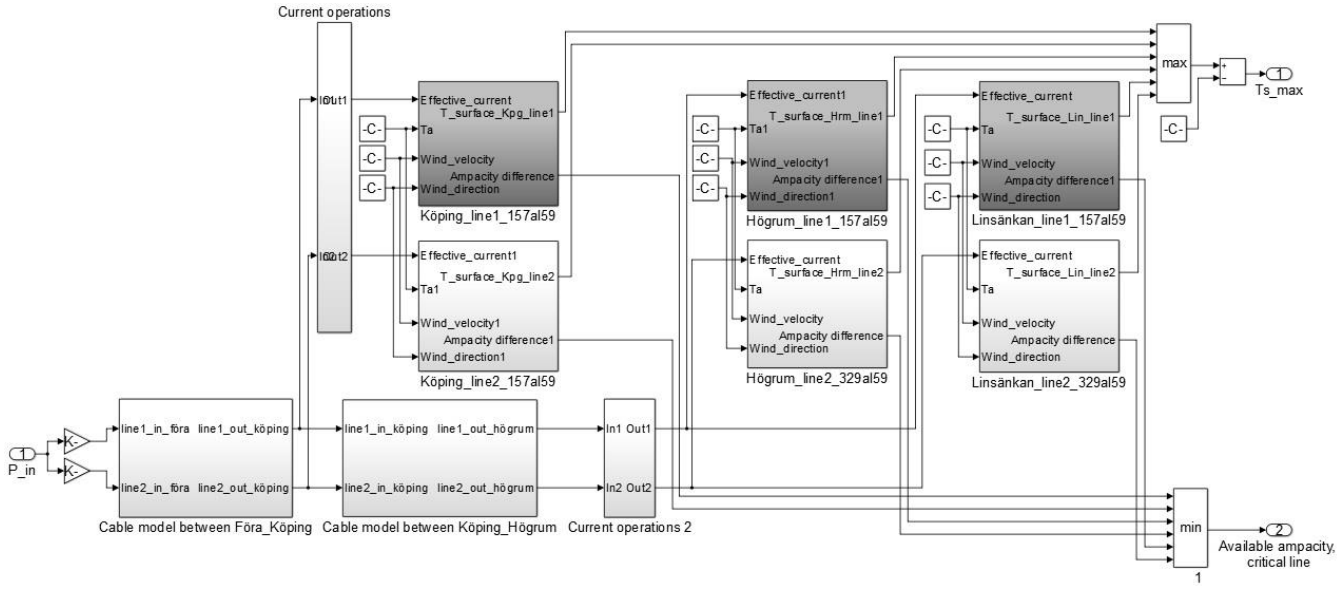

Figure 3-1. Thermal model as seen in Simulink.

The figure shows the model of the larger thermal system, with subsystems containing the individual line stations and the heat balance within them, as well as models of the grid between the three measurement stations. A more in-depth look at those subsystems can be found under the following subheadings.

At the far left of the model is the power input, which is the power in MW coming from Kårehamn. It is divided into two lines, both sharing an equal amount of the power. This signal is fed through the grid models, and then into the six different line models, each representing one measurement station, which can be seen in Figure 3-2. There are two subsystems just before going in to these line models, which contain equations, converting the power value to current and also converting it from alternating to direct current, ultimately sending it into the thermal models. Out from these subsystem come signals containing values both that of the surface temperatures, as well as that of the ampacity differences. The six different temperature values are then compared, and the highest temperature, the most critical, is then selected and sent as an output with which the whole system will be controlled. Values for the ampacity difference are also compared, but there the smallest value is sent out.

To be able to keep track of all the different parameters, and to not have to go through the model doing constant small changes to individual parameters, a MATLAB *m-file* was written. The complete m-file can be studied in Appendix B.

3.1 Individual measuring station

In Figure 3-2 is a picture of the model for the thermal heat balance at an individual lines measurement location. In reality there are two for this model relevant line sections on Öland, but

they only differ in values such as diameter, dc resistance etc., and therefore it is sufficient to only show a figure of one of the two line models, since they are equal in everything except those certain parameters.

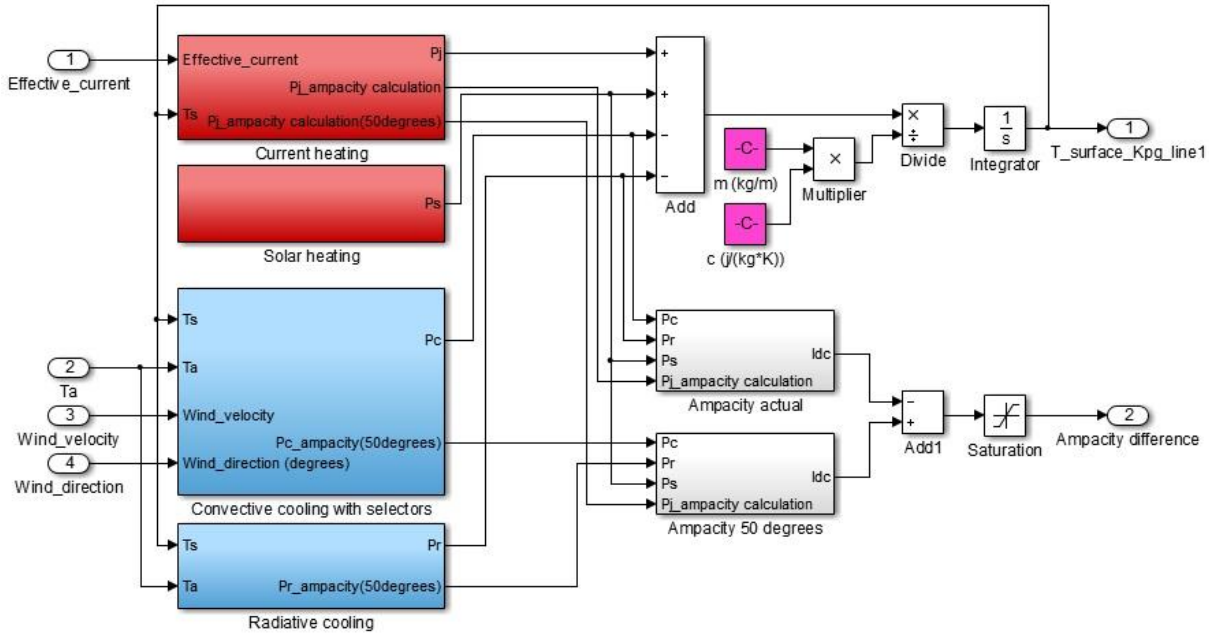

Figure 3-2. Model of individual lines measurement station, as seen in Simulink.

As stated before, this subsystem contains the thermal heat balance, and its main function is to compute the conductor surface temperature, according to the following equation, derived from the equation in section 2.2:

$$T_s = \int \frac{P_J + P_S - P_C - P_R}{m * c} dt$$

The four subsystems contain the different thermal gains, color-coded to be able to easily see if it is a heating gain or cooling gain. They are, in order from top to bottom; current heating, solar heating, convective cooling and radiative cooling. These are added and their sum later divided by the specific heat gain and mass of the conductor. The integrator outputs the surface temperature, and feeds it back into the thermal gains. It requires a selectable starting value. These subsystems contain only mathematical operations, but the “Convective cooling with selectors”-block can be interesting to study further, since its operation depends on several factors, most notably the wind speed on the conductor. Figure 3-3 shows part of that subsystem.

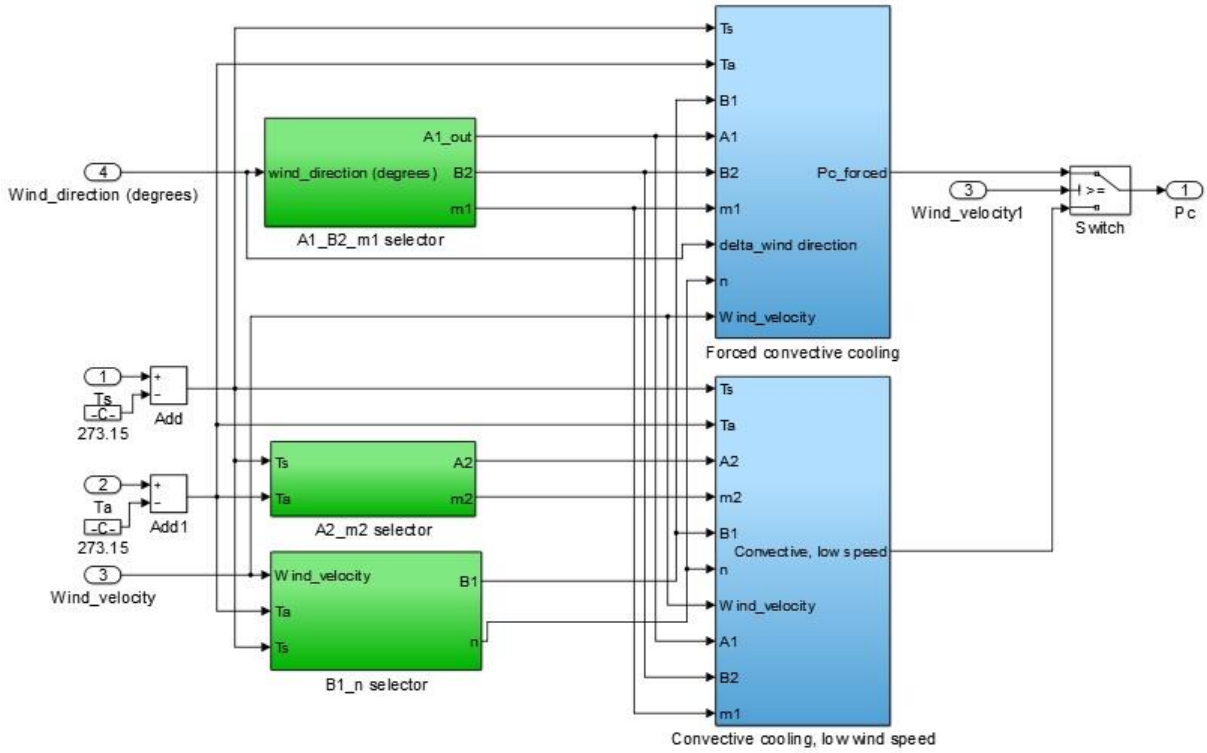

Figure 3-3. Model of part of the convective cooling gain subsystem, as seen in Simulink.

What can be seen in Figure 3-3 is the model of the convective cooling equations in section 2.2.3. There are really two almost identical systems in the model. The second one, outputs a value with an input surface temperature of 50 °C, whilst the one shown in the figure uses the real surface temperature input, fed back from the complete model. Green blocks here contain selectors that select miscellaneous values based on inputs. These equations and the selection criteria can be viewed in section 2.2.3. The blue blocks contain the mathematical equations.

In Figure 3-2 the ampacity is also calculated, and is later used to handle the additional wind and solar power. There are two values for the ampacity, one for the actual surface temperature, and one for the ampacity at a surface temperature of 50 °C. These two values are subtracted and the difference outputted. When the output from Kårehamn is restricted below its maximum, the difference between the two values is zero. When the output from Kårehamn is at its maximum, however, and there is room for more power, this ampacity difference rises above zero. There is a saturation block here as well, to prevent error with ampacity differences below zero.

3.2 Grid model

To simulate the grid on Öland, two blocks with line models were used, so that external power inputs, representing different power generating stations or farms on Öland - and outputs, representing loads - could easily be added to the model. What has been done in this model is basically adding the external power and subtracting the external load. They were assumed to load each of the two lines equally unless stated otherwise. The document [13] provided by E.ON, has been used as a reference for determining how to construct these grid models. Figure 3-4 shows the grid model for northern Öland.

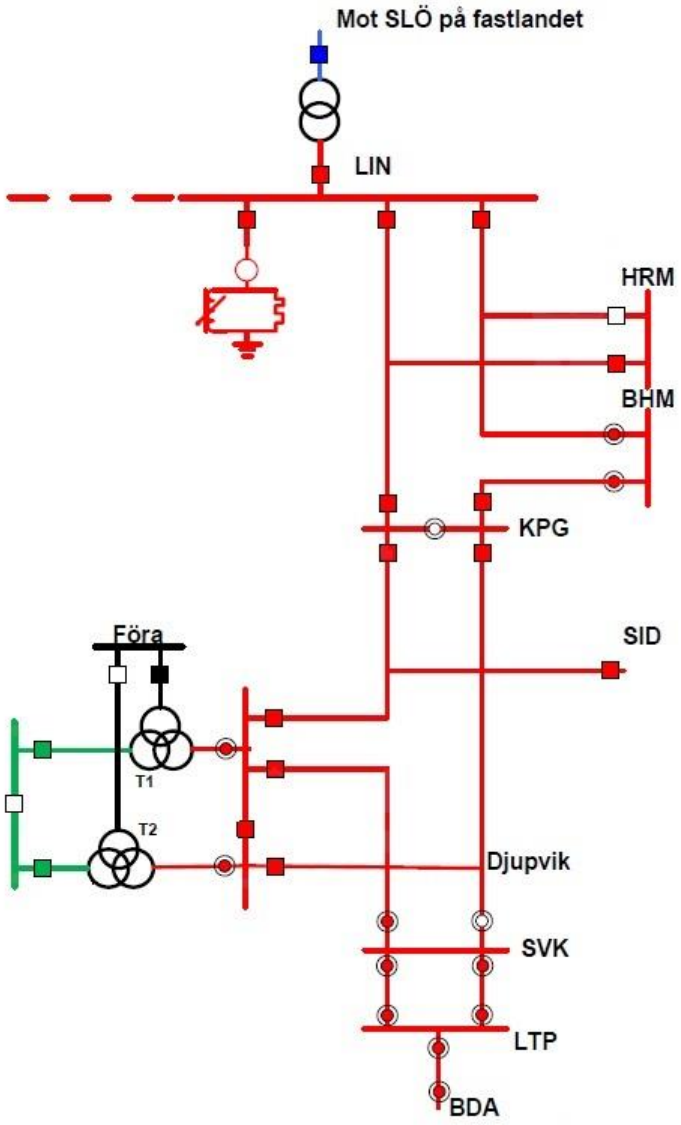

Figure 3-4. [13] A simplified model of the grid on northern Öland.

In the figure, which is a simplified picture of the one found in [13], we can see all the locations on the grid. The picture shows the grid upside down, meaning LIN is the furthest south, while BDA is the furthest north. The green lines represents the connection of Kårehamn to Föra. The stations that are relevant for surface temperature measurments in this thesis are KPG which is Köping, HRM which is Högsrum, and LIN, which is Linsänkan. In truth, these sections are all relevant, as each location is a load and/or contains some form of power generation.

From the same document, the value for all these external power generation units was also taken. The maximal output for these were, which can also be seen in Appendix B, the following:

Wind power Löttorp:	3 MW
Wind power sid:	16 MW
Wind power Köping:	unknown (assumed 0 MW)
Wind power Köping (O62 rail):	20 MW
Wind power Borgholm:	7.7 MW
Wind power Högsrum:	20 MW

These maximal output values were used throughout this thesis. It is impossible that these external sources would output this power constantly, but since they increased the surface temperature if anything and it was thought best to test something more considered worst case, rather than some other lower number or mean output which wasn't known.

As opposed to the wind power feeding the grid, the loads were chosen with a minimal value, for the same reason the max values were chosen for the external power sources. According to the document [14] provided by E.ON, the load on the line varies significantly during the year, even during shorter time spans. The information provided in the document only highlighted the load in a section of the line, rather than the local loads. To find out the local loads, and their minimum, a list was compiled showcasing the difference in load at two sections, for example sections Linsänkan-Borgholm and Borgholm-Köping. From that list the minimum value for the load was selected. This value was close to 0 MW on all places. The exact values can be seen below, or in Appendix B.

Load Föra:	0 MW
Load Djupvik:	$2.75*10^{-4}$ MW
Load sid:	0 MW
Load Köping line 1:	0.76 MW
Load Köping line 2:	$2.09*10^{-3}$ MW
Load Borgholm:	$7.55*10^{-4}$ MW
Load Högsrum:	$1.65*10^{-3}$ MW

As stated, a constant maximum external power feeding the grid as well as a constant minimum load on the grid is hardly plausible - but going forward, it was thought best to have this kind of worst case setup and design the model and control such that it could better handle any difficulties that could arise.

Chapter 4. Verification of thermal model

For verification purposes, the model had to be tested. The first and most obvious way, was to verify it against the many examples in [5]. During verification, a modified model of only one line was used, without all other external loads and wind power, to simulate the line type used in the report as accurately as possible.

4.1 Verification against CIGRE report

The overhead cable used in all of these examples is the *428-A1/S1A-54/7 "ZEBRA"*, which is a conductor with a steel core, surrounded by aluminum.

Its characteristics are [5], [15]:

D = 28.6 mm
d = 3.18 mm
R_{dc}= 0.0674 Ω/km (at 20 °C)

To account for the fact that the cable is aluminum-clad with a steel core, the equation $m * c = m_a * c_a + m_s * c_s$ was used, with the following values:

m_a = 0.43 kg/m
c_a = 481 J/(kg*K)
m_s = 1.16 kg/m
c_s = 897 J/(kg*K)

Characteristics that could not be found, were set according to the Öland case and its conductors. Other values that had to be computed or changed for these tests were:

Gravity of earth:	9.807
Absorptivity of ZEBRA conductor:	0.500
Emissivity of ZEBRA conductor:	0.456

All temperature values and other values in their examples were calculated numerically, whereas the answers produced by the model in this thesis were obtained visually, by looking at the relevant graphs.

4.1.1 Surface temperature calculations for the steady state, example 1

This example calculated the surface temperature of the conductor, with the following parameters:

Global solar radiation:	980 W/m^2
Wind speed:	2 m/s
Wind angle:	45 °
Ambient temperature:	40 °C
Height above sea level:	1600 m
I_{ac}:	600 A

According to the example, the final surface temperature was ca. 58.5 °C. Results from the model showed a surface temperature of 58.9 °C, as shown in Figure 4-1. That's a difference of less than 1 %.

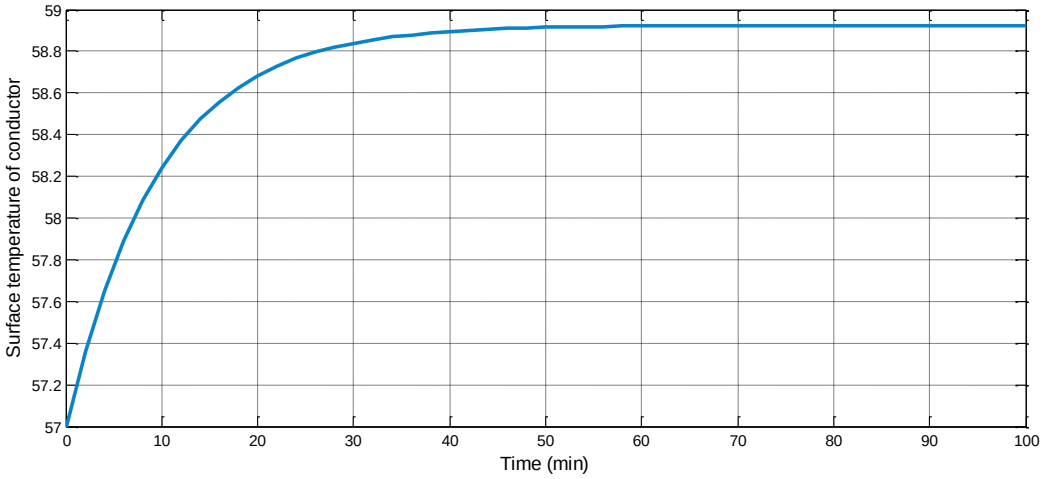

Figure 4-1. Graph showing the conductor surface temperature, from an initial guess of 57 °C.

The curvature of the graph is due to it rising from the, by the system required guess of the initial surface temperature.

4.1.2 Surface temperature calculations for the steady state, example 2

This example is the same as example 1, i.e. the surface temperature is calculated. The difference here is the parameters, which are:

Global solar radiation:	980 W/m^2
Wind speed:	0.2 m/s
Wind angle:	variable
Ambient temperature:	40 °C
Height above sea level:	1600 m
I_{ac}:	600 A

Results from the CIGRE report showed the conductor surface temperature to be 83 °C. The result of this model was a surface temperature of 84 °C. The difference here is roughly 1.2 %, which is shown in Figure 4-2.

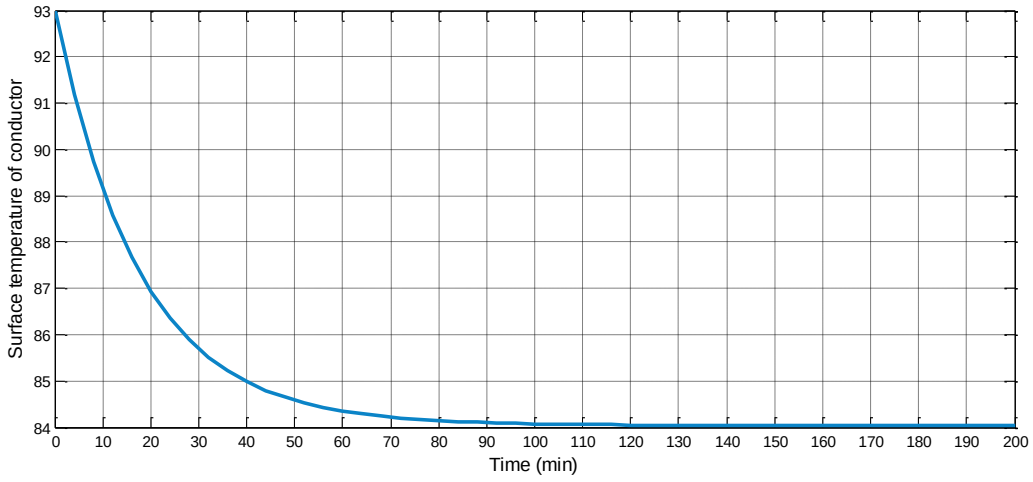

Figure 4-2. Graph showing the conductor surface temperature, from an initial guess of 93 °C.

Since the wind speed in this example is lower than 0.5 m/s, they compared the convective cooling gain using the three different calculations, as discussed in section 2.2.3. They found the value using the equation for natural convection was the largest and was thus used.

4.1.3 Calculations for the unsteady state, example 1

This example tested a current step from 600 A to 1200 A, to show several different results such as thermal time constant, steady-state temperatures etc. They had a maximal allowable temperature of 85 °C. The parameters used in this example were:

Global solar radiation:	980 W/m^2
Wind speed:	see table
Wind angle:	45 °
Ambient temperature:	40 °C
Height above sea level:	300 m
Initial current I_{ac}:	600 A
Final current I_{ac}:	1200 A

Reference results from the example are compiled in Table 4-1, as opposed to the results from the thermal model of this thesis, compiled in Table 4-2.

Table 4-1. [5] Results produced by CIGRE report for unsteady state example 1.

Wind velocity (m/s)	**2.0**	**1.5**	**1.0**	**0.5**	**0.0**
Steady-state temperature θ_{m1} with I_{ac1} (°C)	57.0	59.9	63.4	70.5	83.2
Steady-state temperature θ_{m1} with I_{ac2} (°C)	98.4	107.5	120.3	145.3	166.2
Solar heating (W/m)	14.0	14.0	14.0	14.0	14.0
Joule heating (W/m)	134	138	144	154	164
Thermal time constant during heating (s)	619	713	844	1101	1317
Time to reach 85 °C (s)	701	534	403	237	28.5

Table 4-2. Results produced by the model of this thesis for unsteady state example 1.

Wind velocity (m/s)	**2.0**	**1.5**	**1.0**	**0.5**	**0.0**
Steady-state temperature θ_{m1} with I_{ac1} (°C)	57.0	60.1	63.7	71.0	84.0
Steady-state temperature θ_{m1} with I_{ac2} (°C)	98.0	107.1	119.8	144.8	166.1
Solar heating (W/m)	14.0	14.0	14.0	14.0	14.0
Joule heating (W/m)	131	134	139	149	157
Thermal time constant during heating (s)	601	666	783	973	1004
Time to reach 85 °C (s)	684	501	382	219	15

4.1.4 Calculations for the unsteady state, example 2

This example tested a current drop from 900 A to 200 A. All of the other parameters were the same as in the previous example, except here they had a maximal allowed temperature of 70 °C. The CIGRE report results are shown in Table 4-3, results from the thermal model used in this thesis in Table 4-4.

Table 4-3. [5] Results produced by CIGRE report for unsteady state example 2.

Wind velocity (m/s)	2.0	1.5	1.0	0.5	0.0
Steady-state temperature θ_{m1} with I_{ac1} (°C)	72.7	78.3	85.4	99.5	117.2
P_1 (W/m)	82.3	83.6	85.2	88.5	92.6
P_2 (W/m)	17.0	17.0	17.0	17.0	17.0
Thermal time constant during cooling (s)	520	597	691	867	1071
Time to reach 70 °C (s)	57	190	380	824	1479

Table 4-4. Results produced by the model of this thesis for unsteady state example 1.

Wind velocity (m/s)	2.0	1.5	1.0	0.5	0.0
Steady-state temperature θ_{m1} with I_{ac1} (°C)	72.7	78.4	85.5	99.9	117.9
Thermal time constant during cooling (s)	525	586	693	875	1070
Time to reach 70 °C (s)	71	207	395	864	1909

4.1.5 Conclusion and discussion on verification

From what can be seen, the results from the first two tests, section 4.1.1 & 4.1.2 closely agrees with the result from the report. As mentioned, the curvature in Figure 4-1 and Figure 4-2 is just the surface temperature correcting from an initial guess. We can see that they have reached steady state temperatures after approximately 60 and 100 minutes respectively.

The results from example 1 and 2 in appendix 2 with the unsteady state however, differ quite a bit in some aspects, notably the time it takes to reach the maximal allowable temperatures, as well as the thermal time constants. As stated before, results from the thermal model were all obtained visually whereas in the CIGRE report, they were all calculated numerically.

When it was calculated numerically as well with the steady state temperatures from simulation results, the numbers much more closely resembled what their results showed - for example a thermal time constant of 1125 and 1354 seconds, with wind speeds 0.5 and 0.0 respectively, compare Table 4-1 and Table 4-2. Errors from visually obtaining the results were surely present, even though they were carefully obtained, and would certainly not result in a difference of 10-30 % as it was in a few cases. This could probably mean there is some error in the way the thermal time constant is calculated, but when checked against the equations in sections 2.3 and 2.4, which were taken from said report, the results were in line with its.

4.2 Testing the thermal model

When the verification against the *CIGRE* report was completed and it was shown that the model of the thermal heat balance worked as intended, it was time to modify its parameters and establish that it would perform correctly or rather as expected, before moving forward and tailoring it around the Kårehamn and Öland case. Two tests were carried out, both with changing power, a current step. This was meant to resemble a change in the output from Kårehamn, as a way to see how the surface temperature of the conductors, at all six stations, behaved.

4.2.1 Output change: 35- 48 MW, no loads

In this initial test, a power output increase from 35 MW to 48 MW was simulated, in which Kårehamn goes from a less than maximal output, to full output. The location-specific parameters were taken arbitrarily to resemble a normal spring or summer day and their values can be seen below, other fixed parameters in the m-file in Appendix B. The initial guess for the temperature here was 40 °C.

Wind Speed Köping:	6 m/s
Wind direction Köping:	5 °
Ambient temperature Köping:	19 °C
Wind Speed Högsrum:	6.5 m/s
Wind direction Högsrum:	85 °
Ambient temperature Högsrum:	21 °C
Wind Speed Linsänkan:	6.5 m/s
Wind direction Linsänkan:	85 °
Ambient temperature Linsänkan:	22 °C

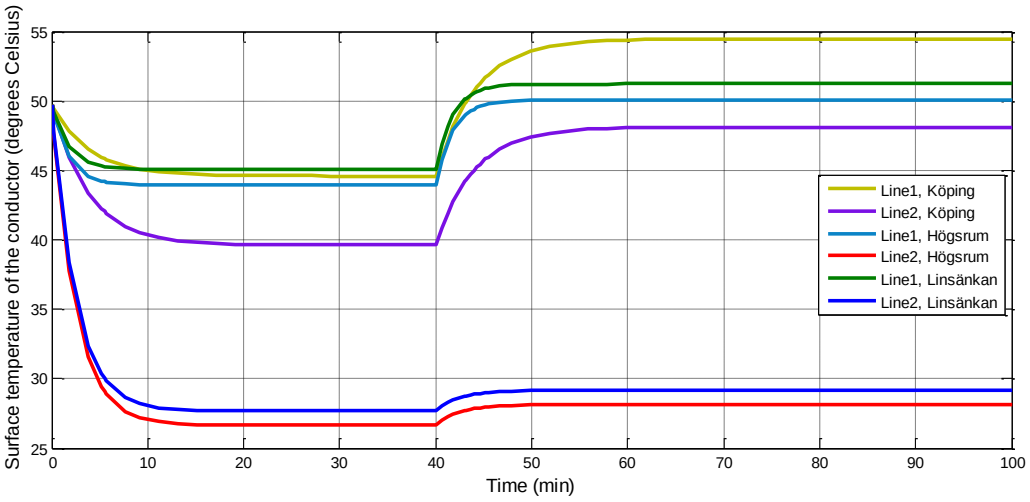

Figure 4-3. Graph showing the change in surface temperature, due to a change in power input.

From Figure 4-3 we can see that the surface temperatures settle in the start after the initial guess. It can be seen that line 2 at both Högsrum and Linsänkan have a considerably lower temperature, compared to the rest. That is due to the fact that that line section is of the type 329 Al59, whereas the others are 159 Al59. Since they have a much larger diameter, but are still carrying the same current, their surface temperature is colder. As a result, they don't react as strongly to the power step either.

At the time of 40 minutes, we can see that the surface temperature at all six locations rise, as is to be expected. They all have a thermal time constant varying between approximately 2-4 minutes. The line 1, at Köping, has the highest surface temperature and is thus most critical. This is due mostly to the chosen parameters, with a slightly lower wind speed, but particularly because of the wind direction that is almost parallel to the line, causing the wind to cool it much less effectively.

Three of the lines have a surface temperature above 50 °C, even though the weather parameters are not particularly high. The reason the surface temperature exceed 50 °C is most likely due to all the external power acting on the grid, driving the general surface temperature up, which is discussed in section 3.2.

4.2.2 Output change: 48-0 MW, no loads

In this simulation, Kårehamn gets completely shut off. That means the output goes from 48 MW to 0 MW. The location-specific weather parameters used here were the same as in the previous simulation.

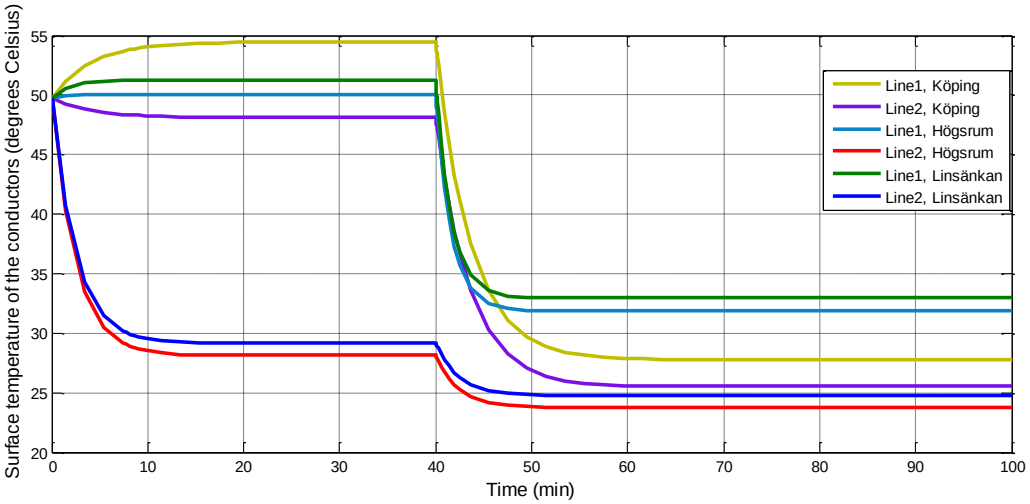

Figure 4-4. Graph showing the change in surface temperature, due to a change in power input.

Here too, we can see the initial settling of the surface temperatures from the initial guess at the start. They should be expected to have the same steady-state temperature as that of the lines in Figure 4-3 after the power increase, as they do. After the power change at time 40 minutes, the surface temperatures all drop, which is expected. One would expect they drop to about ambient temperature when Kårehamn doesn't deliver power. They don't, and that is partly because of external power feeding the grid.

4.3 Impact of solar irradiation

No solar irradiation measurement equipment is currently installed or planned to be installed at any of the measurement locations. However, the thermal heat balance and the model use solar radiation as part of its equations. This led to the question if it should be included in the model going forward at all.

To get a better picture of the significance that solar radiation has on the surface temperature of the overhead conductors using the simplified method in section 2.2.2, simulations with and without solar heat gain were made. These simulation results can be seen in Figure 4-5 and Figure 4-6.

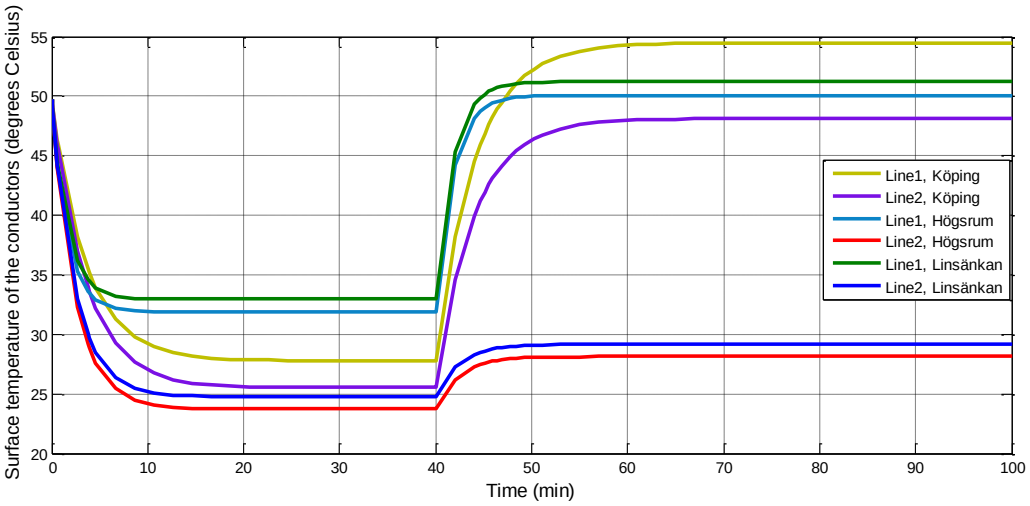

Figure 4-5. Graph showing the surface temperature of the conductor with solar gain calculations included.

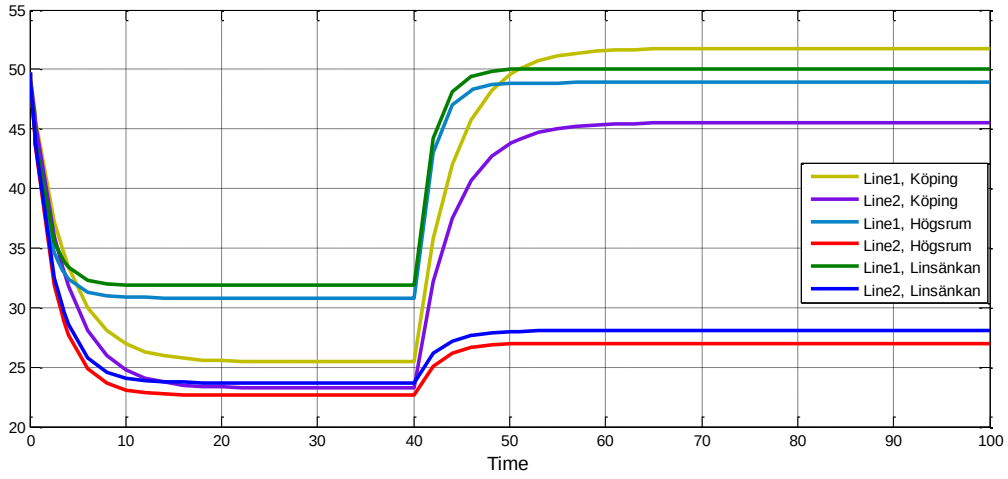

Figure 4-6. Graph showing the surface temperature of the conductors without solar gain calculations.

The significance of the solar heat gain depends largely on the value of the other parameters in the heat balance, but when looking at the resulting graphs from these simulations, it was clear it had an impact; which was in the magnitude of about 2-3 °C. When viewed against the rest of the parameters affecting the heat balance, it was clear it was impacting, at least to some degree. Current heating and convective cooling were the largest by far, but the solar heating was quite often as large as, or sometimes larger than, the radiative cooling. The radiative cooling gain used here however, has a very small value for the chosen emissivity of the conductor, and it is true it would be larger in the case of a higher value for the emissivity.

As it was affecting the surface temperatures a few degrees and the fact it was as significant in terms of value as the radiative cooling, it felt necessary to include solar irradiation in this model. Also considering it would set the model on the “safe side” as it was yet another case worse with it included. The solar heating was designed using the highest global irradiation according to section 2.7, but it could be argued that one could use it with a mean value, or any lower value.

Chapter 5. Controlling the thermal model

The purpose of the control is to make sure the surface temperature of the conductor with the most critical temperature, and therefore any conductor, does not exceed 50 °C. A controller was implemented into the Simulink model to meet that end. The complete system with feedback and control can be seen in Figure 5-1.

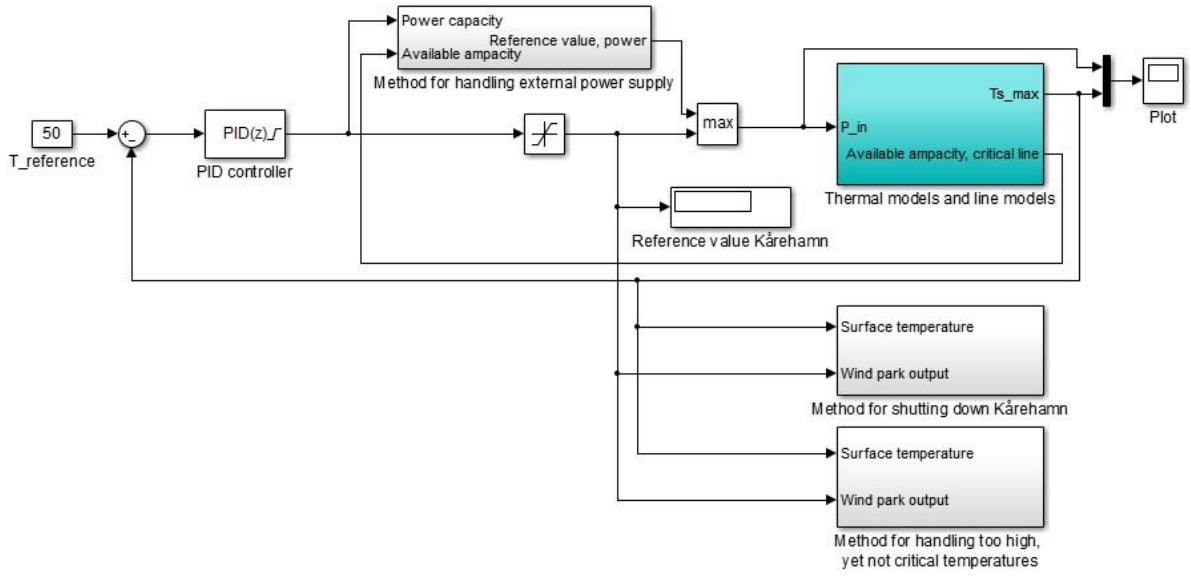

Figure 5-1. The complete Simulink model, with temperature control and error handling.

Here we see the output from the thermal model, the surface temperature, is compared with the reference temperature of 50 °C, and the resulting difference is then fed into the PID controller. Out from the controller comes a value in MW, which in turn is fed into the thermal model. This value, which goes through the saturation block, will be sent to Kårehamn, since it is the reference value for its output. Additionally there are three more blocks which will be explained and discussed later in this report, methods for error handling and additional generation units.

The main task for the controller is to eliminate the error in temperature, and thus only an I-regulator is essential. Short periods of temperature over 50 °C is allowed, so overshoots at regulation is nothing to worry about unless they become significant. Back-calculation anti-windup was implemented to help partly solve this problem and limit the overshoot. Implemented into the controller was also saturation of the output with a lower limit of 0 MW, and an upper limit of what the wind farm can deliver.

5.1 Tuning the controller

Implementing an I-controller only, did in fact regulate and control the system. However, it wasn't very fast and sometimes it gave quite significant overshoots. Not critical for the real case perhaps with overshoots of up to 10 °C, but enough to make it desirable to further tweak it. A full PID controller was tried, but at first it seemed impossible to choose a set of parameters, especially considering the optimal configuration changed depending on the simulation and all parameters involved. The PID controller block can as mentioned before, be seen in Figure 5-1 to the left.

Simulink has an automatic tuning tool that proved useful. It was decided to tune the controller for the slowest case. This would ensure a stable, albeit a bit slower, response and control of every other

case. Looking at the examples in the CIGRE report, specifically example 1, Appendix 2 as seen in section 4.1.3, it was clear that a large current step increase with no wind on the conductor was the slowest case. A temperature drop from +40 °C and -20°C on the model in this thesis would give a large current step for which the regulator could be tuned. The simulation was set to run its course, and when it had finished, the tuning tool was used. The response time was altered somewhat, to give an overall satisfying set of parameters. These parameters were rounded off to slightly different numbers, so as to make it more intuitive and not have several significant digits. The chosen parameters can be seen in the table below.

	Value
Proportional gain	4.5
Integral gain	0.0075
Derivative gain	-135
Filter coefficient	0.03

The first three parameters constitute the P, I and D gains, and the Filter coefficient is a parameter which specifies the pole location of the filter in the derivative action.

Below is a picture showing the tuning tool. The blue curve represents the response with the suggested parameters, the grey with the existing parameters.

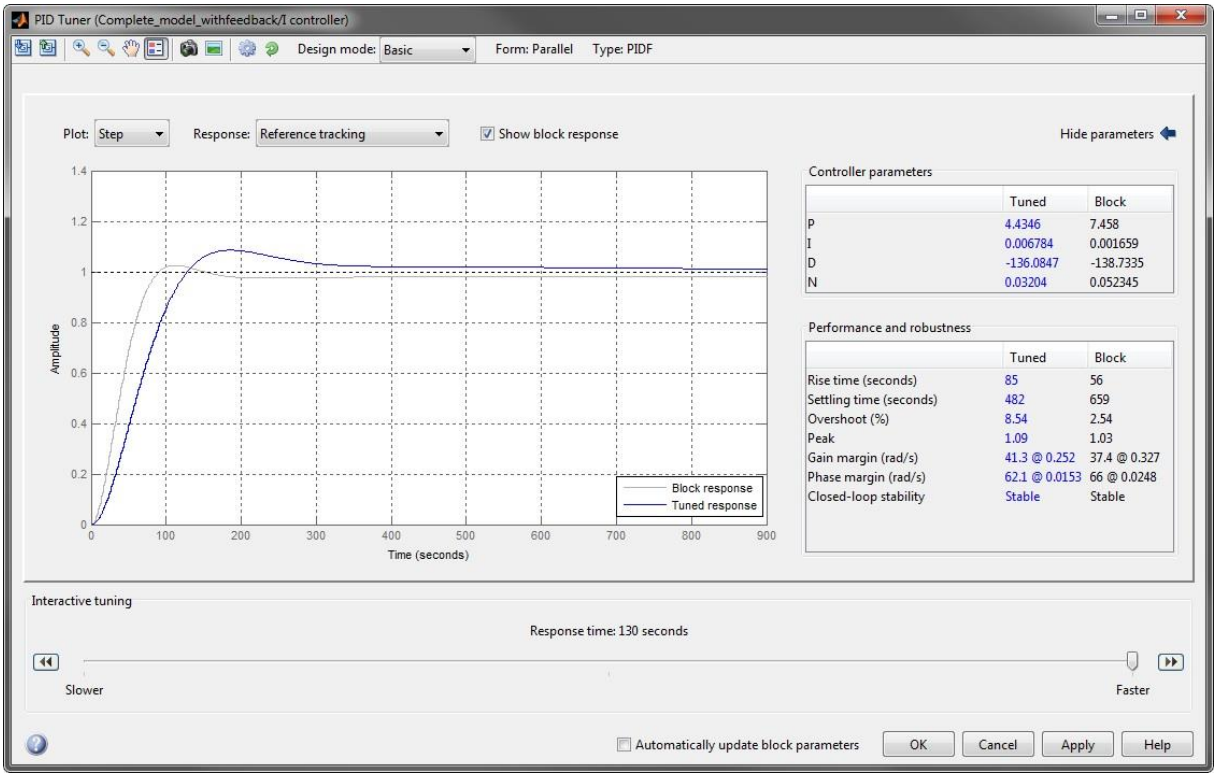

Figure 5-2. Tuning tool and step response for large temperature drop.

To make sure it worked as intended for the faster case – a slower but more stable response – the chosen parameters were tested for a current ramp instead of a step, and with a high wind speed acting on the conductor. The results of the tuning tool in that case can be seen in Figure 5-3. There it can be seen that the grey curve is the chosen parameters, and that it is slower and more stable, with no overshoots. To further validate the parameter choice, the suggested parameters in Figure 5-3 was

chosen as the new, and the tuning tool tried on the previous case with these parameters. The results of that simulation can be seen in Figure 5-4. There it can clearly be seen, had these parameters been chosen as the ones used for all cases, it would be faster, but would give much larger overshoots in the step response.

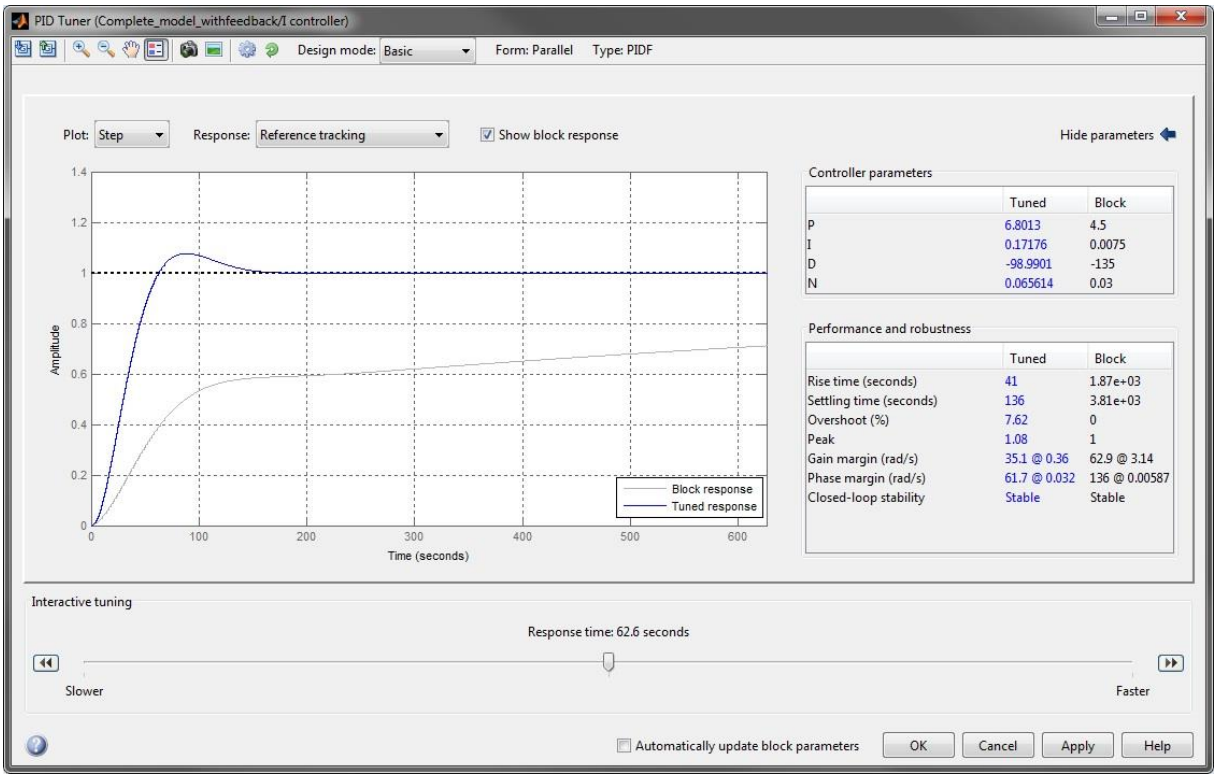

Figure 5-3. Step response with the chosen parameters for a different case, faster case.

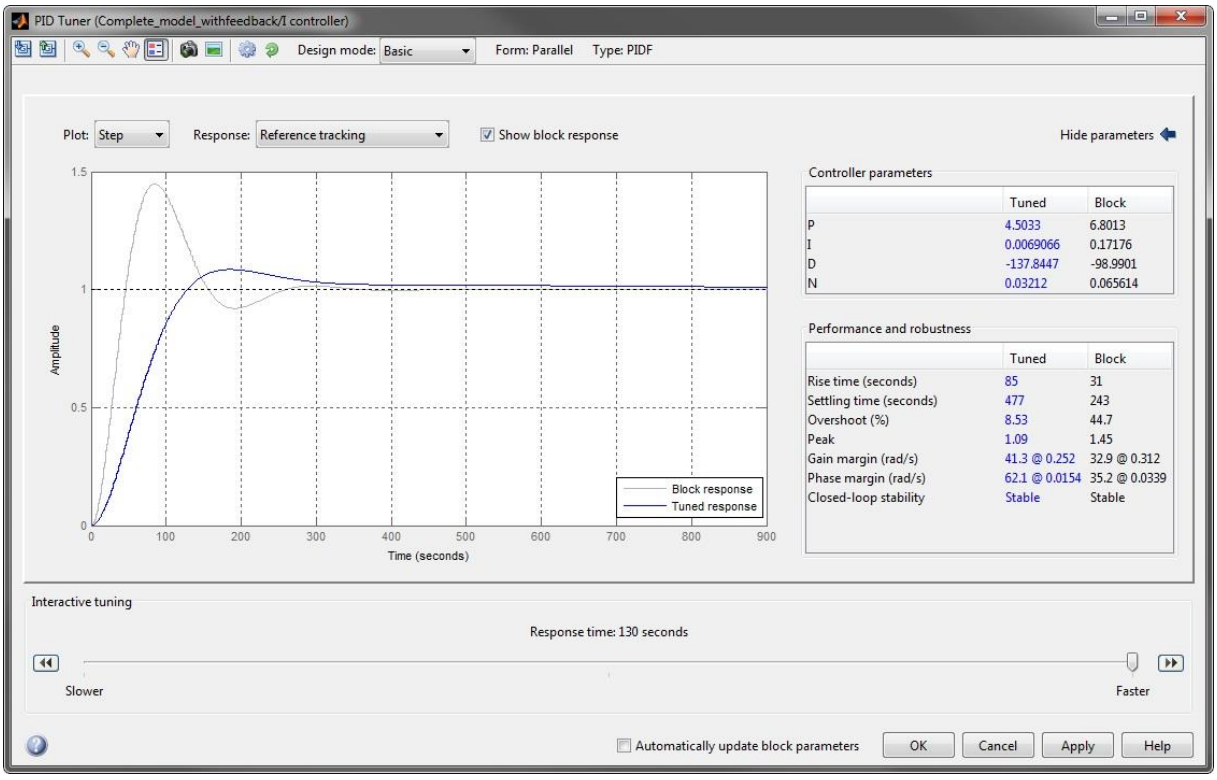

Figure 5-4. Step response, with different parameters based of previous simulation, for the slowest case.

5.2 Simulations with control

To test the model and control of it, different simulations had to be made. It was desirable to test the model in several different situations, with different and changing parameters affecting the conductor temperature directly. Changing wind speed, wind direction and ambient temperature at measurement locations were the chosen parameters, since they are the only ones likely to change in the real case (except the current, but that is a consequence of the control). These weather parameters are the ones that affect the relevant line sections and their surface temperatures, and may not coincide with the ones at Kårehamn. That is to say, testing the model with a specific wind speed does not necessarily mean the wind speed is the same at Kårehamn.

Signals containing step changes and ramp changes were tested. These signals were constructed using the Simulink signal builder, and though not identical, they were all designed so that each signal contained both a positive and negative step and ramp. It was also designed such that the step change and ramp change would differ with positive and negative change, to show the difference in how the system is controlled. Changing values in a ramp rather than step closer resembles the real conditions, but step changes better showcase how the system controls the temperature and the stability of the system. For each simulation, the constant parameters (i.e. two of the three mentioned) were set to extreme values, to show the differences, whilst the third parameter was changing throughout the simulation. Although the signal shows the time in seconds, the simulation results are shown in hours, to make it more intuitive.

These extremes would serve as the worst and best case scenarios and they were: 0 m/s and 15 m/s for the wind speed on the conductor, -20 °C and 40 °C for the ambient temperature, as well as 0 and 90 ° for the wind direction in relation to the conductor direction.

It should be reminded that these simulations not only include the power from Kårehamn which can deliver no more than 48 MW, but also the external power generating units acting on the grid as well as local loads that drive up the surface temperatures in many cases. This is further mentioned in the relevant simulations.

5.2.1 Changing wind speed on the conductor

The signal used for simulating the changing of the wind speed while keeping both the wind direction and ambient temperature at constant values can be seen in Figure 5-5.

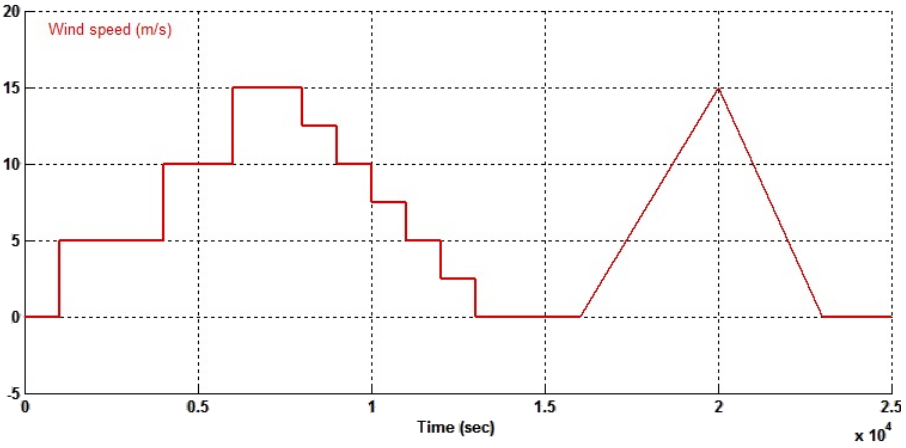

Figure 5-5. Signal used to simulate varying wind speeds.

As can be seen, the signal starts with no wind and then goes up to 15 m/s in steps of 5 m/s. At time 8000 seconds, it again descends, this time in a step with smaller decrements. This process is later repeated with a ramp change. This signal is built so that it is given time to stabilize at times 1000 seconds and 13000 seconds. That is because there the thermal model changes for the wind speed at 0.5 m/s, according to what is described in section 2.2.3. It is thus interesting to see how the model behaves here.

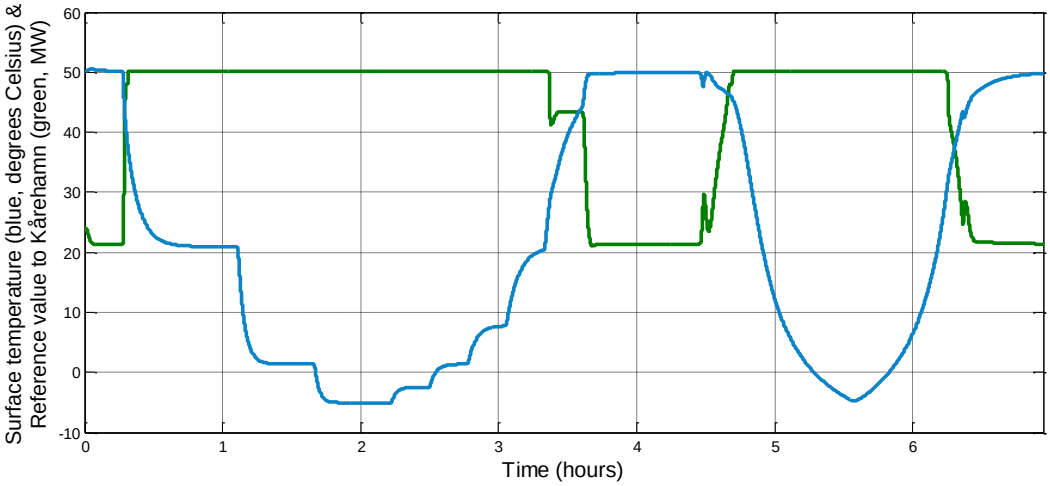

Figure 5-6. Result of simulations, for varying wind speed at conductor, with 0 degrees wind direction and -20 °C ambient temperature. The blue signal shows the surface temperature of the conductor in °C, the green the reference value to Kårehamn in MW.

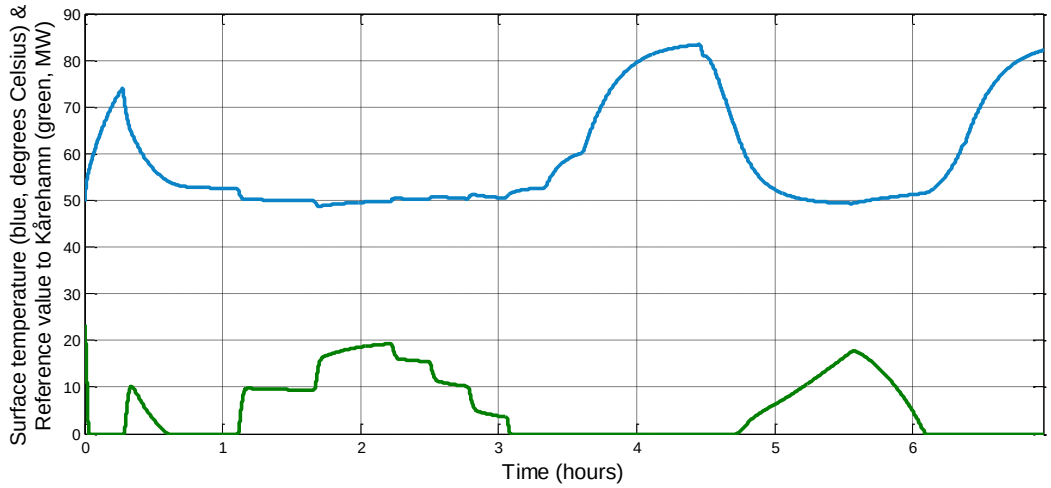

Figure 5-7. Result of simulations, for varying wind speed at conductor, with 0 degrees wind direction and 40 °C ambient temperature. The blue signal shows the surface temperature of the conductor in °C, the green the reference value to Kårehamn in MW.

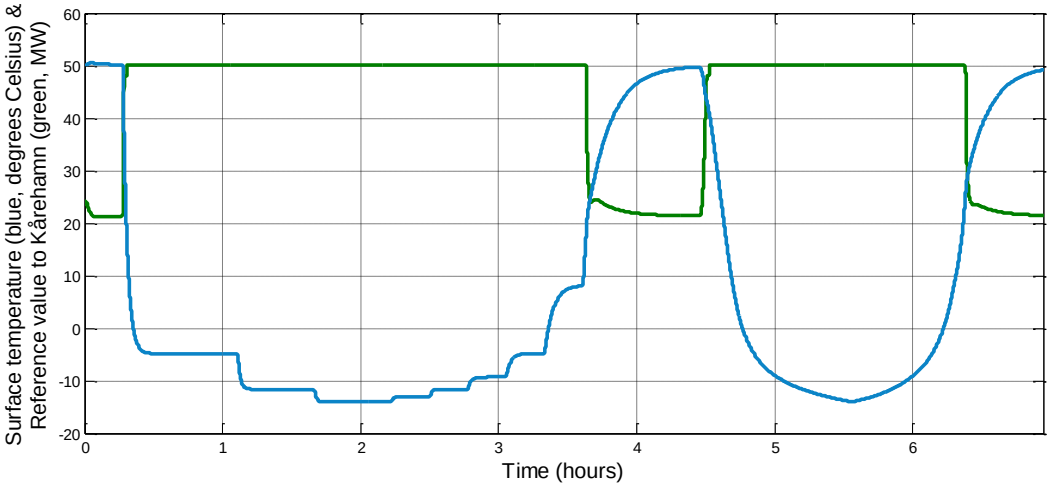

Figure 5-8. Result of simulations, for varying wind speed at conductor, with 90 degrees wind direction and -20 °C ambient temperature. The blue signal shows the surface temperature of the conductor in °C, the green the reference value to Kårehamn in MW.

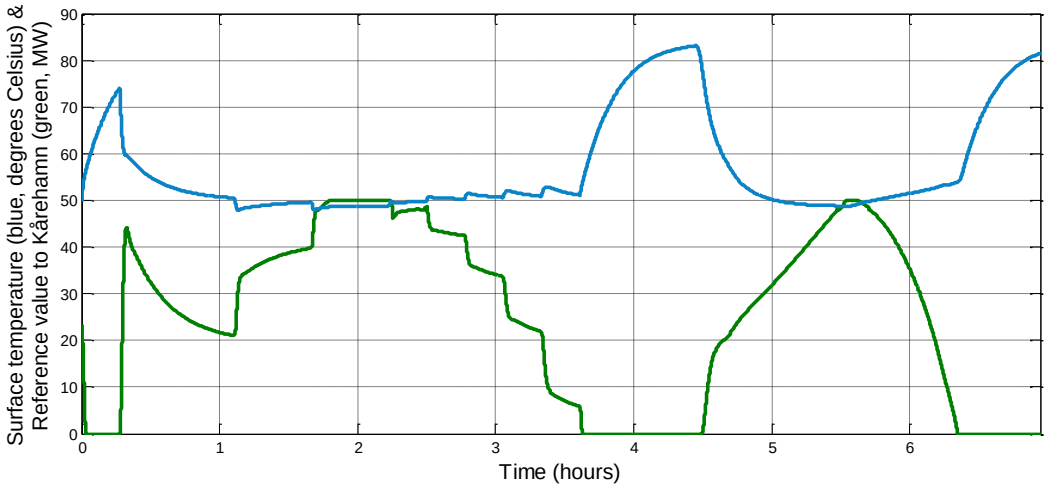

Figure 5-9. Result of simulations, for varying wind speed at conductor, with 90 degrees wind direction and 40 °C ambient temperature. The blue signal shows the surface temperature of the conductor in °C, the green the reference value to Kårehamn in MW.

From all the pictures above, we can see that the wind speed has a profound effect on the surface temperature of the conductor. We can clearly see the temperature is highest with no or little wind, right at the beginning as well as at around four hours into the simulation. This means the reference value for Kårehamn is at its lowest, and in the cases with 40 °C ambient temperature, very low or completely shut off. The two simulations with an ambient temperature of -20 °C have no problem keeping the temperature within its regulation temperature, though the reference power value has to adjust at times when the wind speed drops to 0.

We can also see in the cases with high ambient temperature, the surface temperature of the conductors soars with little wind. This is, as stated many times before, due to external power on the grid. There are no real surprises in these simulations, although the most interesting parts are when the wind power crosses 0.5 m/s, which is especially apparent in Figure 5-6 at just before four hours, five hours and just after six hours into the simulation.

5.2.2 Changing wind direction in relation to conductor

The signal used for simulating a change in the wind direction while keeping both the wind speed and ambient temperature at constant values can be seen in Figure 5-10.

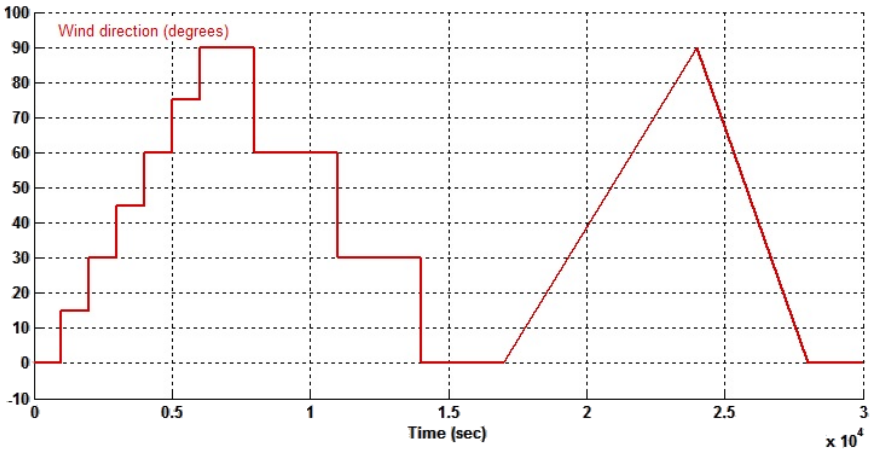

Figure 5-10. Signal used to simulate varying wind directions.

The signal used here starts with a positive ladder from 0 to 90 degrees, with 15 degrees increments. Then it goes down to 0 degrees, in 30 degrees decrements. At the second half of the simulation there are two ramp changes, with different inclinations.

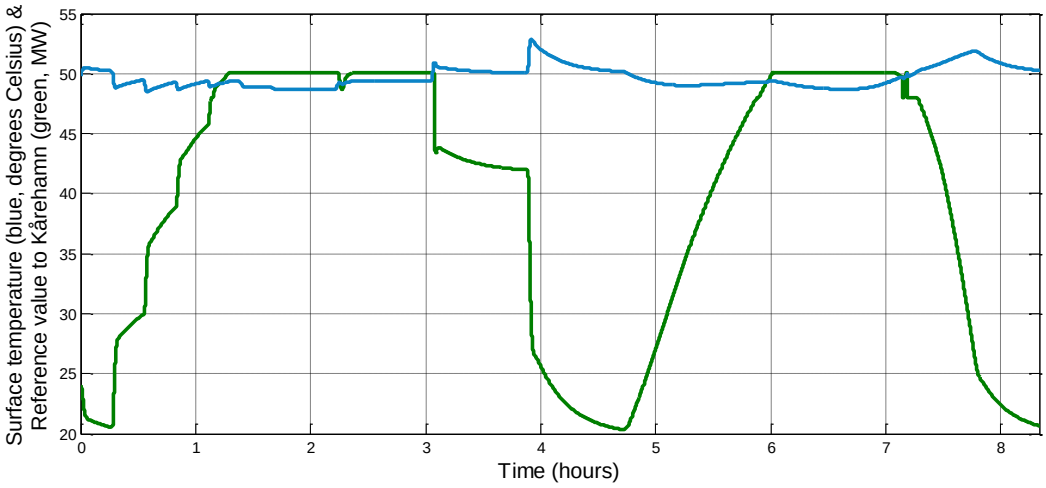

Figure 5-11. Result of simulation, for varying wind direction on conductor, with 15 m/s wind speed and 40 °C ambient temperature. The blue signal shows the surface temperature of the conductor in °C, the green the reference value to Kårehamn in MW.

The simulations with changing wind direction showed that its impact is not quite as significant as the wind speed on the conductor, though it definitely affects how effectively the wind cools the conductor. The three first simulations; two with no wind and different ambient temperature, and one with a wind speed of 15 m/s and -20 °C ambient temperature, are not shown in pictures, since their results were uninteresting with pretty much steady state values regarding the reference value. With no wind, the reference signal being sent to Kårehamn was either 24 MW or 0 MW, at -20 °C and 40 °C ambient temperature respectively. With full wind speed, and low temperature, the reference value was at its maximum constantly.

Figure 5-11 is more interesting however, and we can clearly see the effect on the direction of the wind cooling the conductor. As expected, the cooling effect of the wind is best when perpendicular to the conductor. There is, except small overshoots at just before four and eight hours in the

simulation, no problem for the model to keep the surface temperature within regulation temperature. It is also interesting to note the external power sources connecting and disconnecting, visible shortly after seven hours.

5.2.3 Changing ambient temperature at conductor location

The signal used for simulating a change in the ambient temperature while keeping both the wind speed and wind direction at constant values can be seen in Figure 5-12.

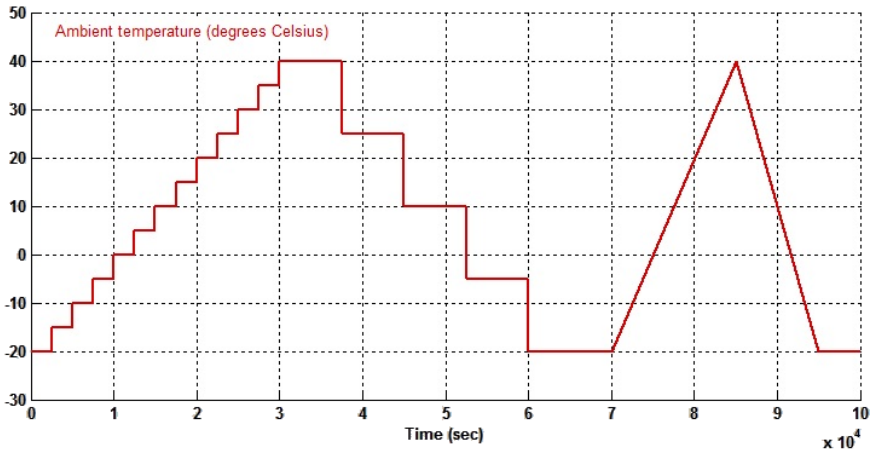

Figure 5-12. Signal used to simulate varying ambient temperature.

The signal and appearance of the signal for the ambient temperature should come as no surprise as it is very similar to the two previous, albeit with a slightly higher inclination of the ramp changes.

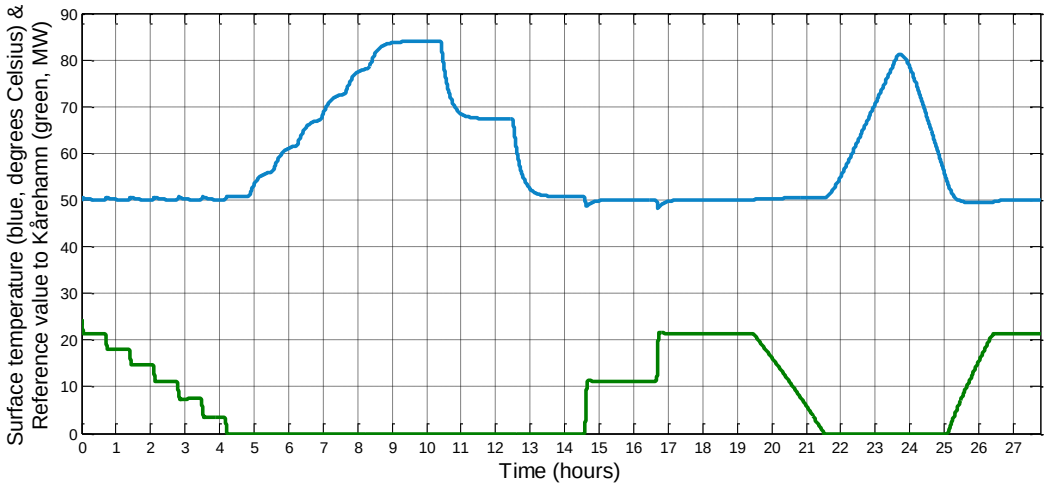

Figure 5-13. Result of simulation, for varying ambient temperature at conductor, with 0 m/s wind speed and varying wind direction. The blue signal shows the surface temperature of the conductor in °C, the green the reference value to Kårehamn in MW.

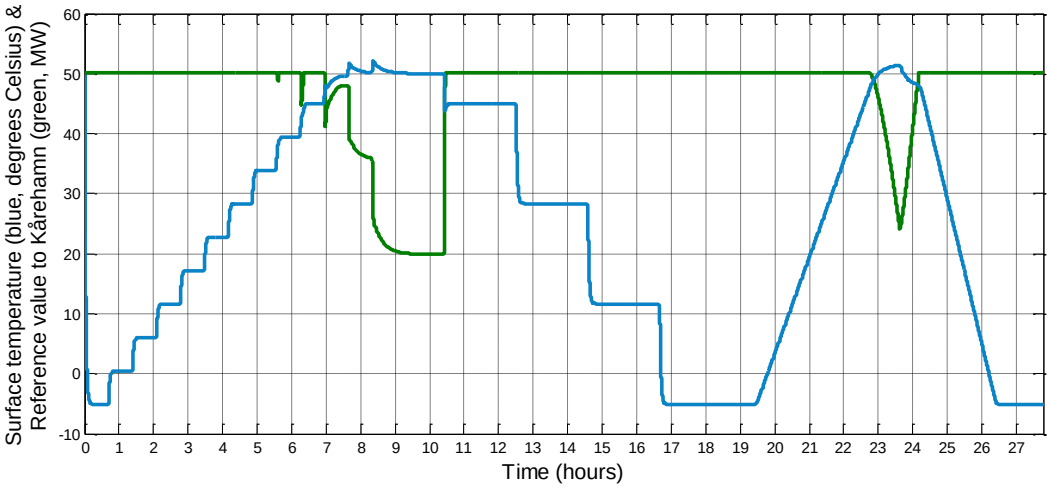

Figure 5-14. Result of simulation, for varying ambient temperature at conductor, with 15 m/s wind speed and 0 degrees wind direction. The blue signal shows the surface temperature of the conductor in ℃, the green the reference value to Kårehamn in MW.

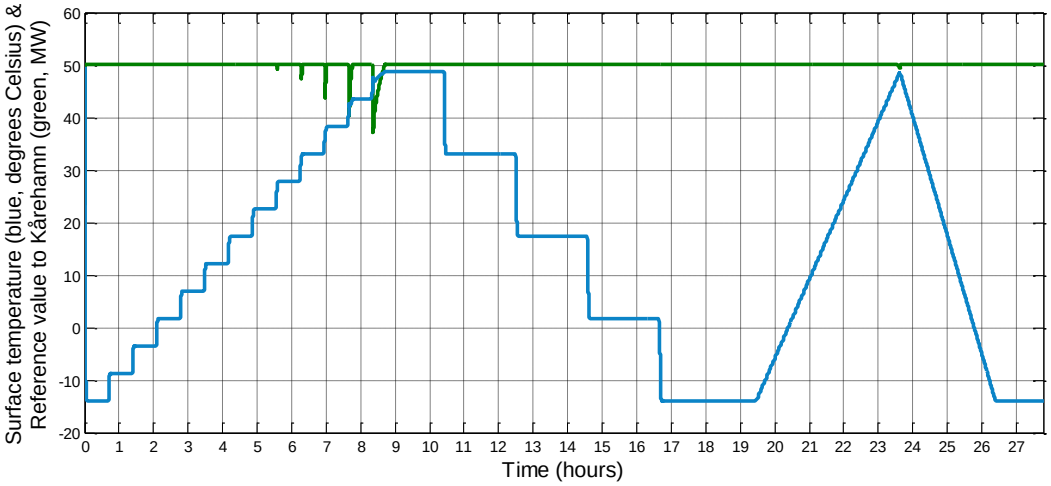

Figure 5-15. Result of simulation, for varying ambient temperature at conductor, with 15 m/s wind speed and 90 degrees wind direction. The blue signal shows the surface temperature of the conductor in ℃, the green the reference value to Kårehamn in MW.

Figure 5-13 shows the simulation result when there is no wind. Varying the wind direction when there is now wind, does not change anything. Therefore, those two first simulations produced the same results. The two latter simulations share a similar appearance, and the effect of the wind direction can clearly be seen. We can see that with a wind speed of 15 m/s, the ambient temperature in this case becomes critical at about 30 °C, and then the reference value has to change. Additionally, with a wind direction perpendicular to the conductor, Kårehamn is at its maximal output almost all the time, except small dips between six and nine hours, which happens because of the derivative part of the control, the system “braces” for a step change that could push the temperature up.

Chapter 6. Alternative incremental control

A secondary objective in this thesis was the modeling of an alternative control method currently used by E.ON, where the surface temperature would be controlled by changing the reference signal in steps, with a set wait time between changes. There were several different flowcharts given; for controlling the current, the temperature as well as handling errors. Since this thesis and the model are limited to controlling the temperature, it was natural to test only their temperature regulation. Current control would be similar, just with a different setup in the model so that the ampacity and ampacity difference would be controlled, i.e. as input into the PID controller.

The method of this control was that the reference value to Kårehamn should be changed in small increments - as opposed to continuously changing as in the controller developed in this thesis - whilst waiting a set period of time in between reference value changes so that they could be sent and to allow for the temperature to change. By default, the number by which the reference value was to be changed each iteration, was 1 MW with a 30 second delay between changes. The modified system to accommodate this can be seen below, in Figure 6-1.

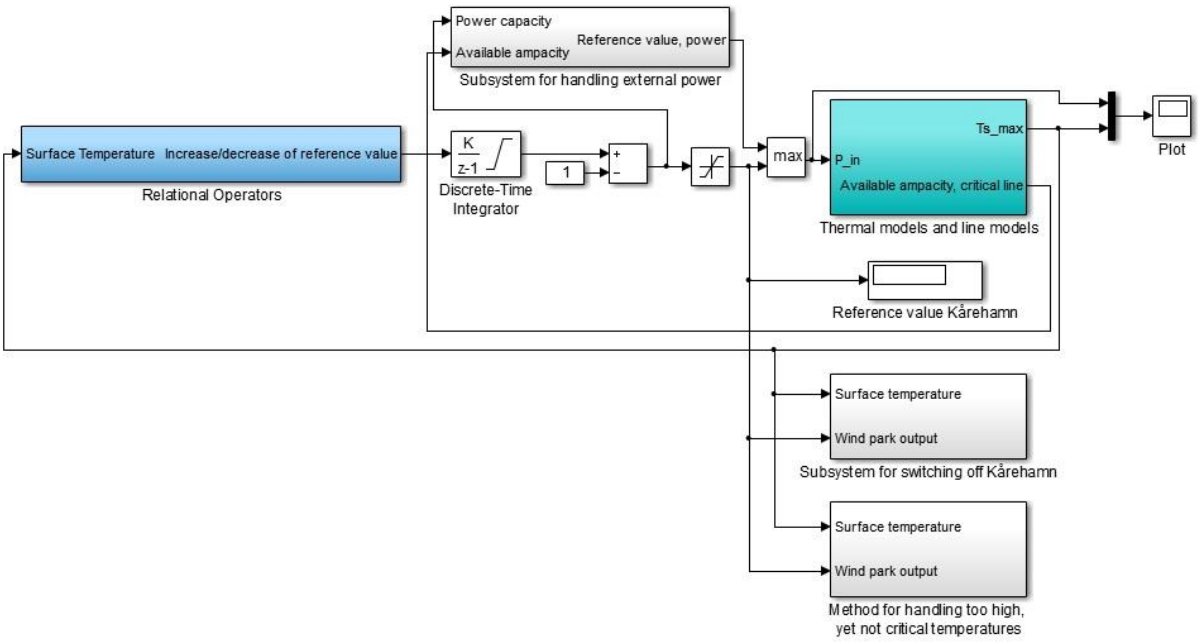

Figure 6-1. The complete Simulink model based with alternate control.

The difference between this model and the main regulated model in Figure 5-1 is the addition of the subsystem named “Relational Operators”, as well as an integrator. The Relational Operators subsystem can be seen in Figure 6-2. The flowchart stated that only when the temperature is higher than 50 °C or lower than 49.5 °C, the regulation be instated. That is what this subsystem checks; if the temperature needs to be corrected. If the surface temperature is below 49.5 °C it outputs 1 and if it is higher than 50 °C, -1. This number, 1 or -1, is then fed into the integrator, which in turn changes the reference value by a positive or negative increment. Inside the integrator, both the size of the change of the reference value and the wait time is given. The minus 1 mathematical operation in Figure 6-1 is because the integrator had to be given a lower saturation limit of 1 instead of 0 to avoid an error.

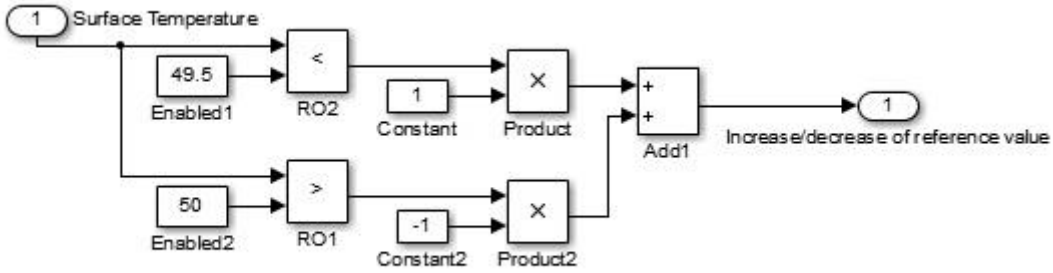

Figure 6-2. Subsystem with relational operators for handling changes in reference value.

6.1 Simulations

The purpose of implementing the alternative control method was to test it against the continuously regulated system built for this thesis. Therefore, it was natural to run the same type of simulations on the model in Figure 6-1, as those done in section 5.2. The three signals used in simulations can be seen in chapter 5 (Figure 5-5, Figure 5-10 & Figure 5-12).

6.1.1 Changing wind speed on the conductor

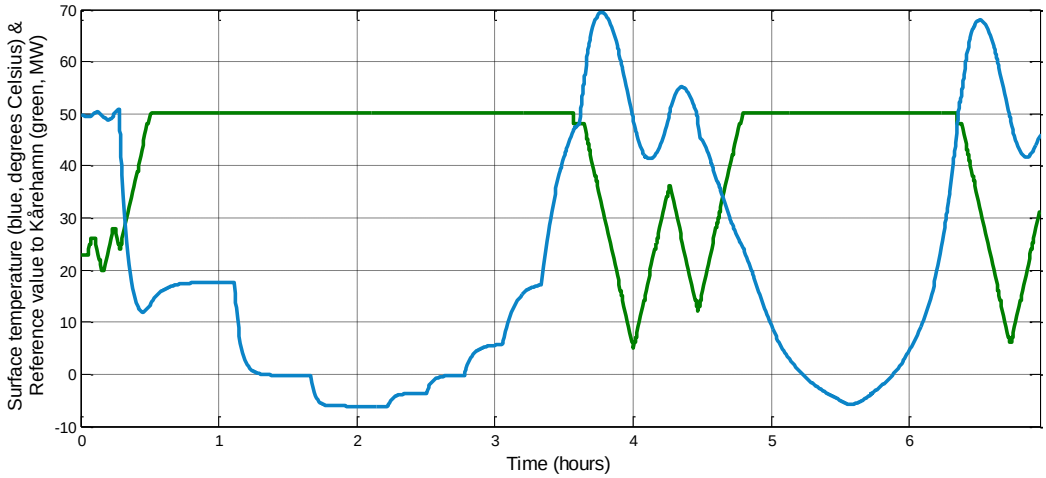

Figure 6-3. Result of simulation, for varying wind speed at conductor, with 0 degrees wind direction and -20 °C ambient temperature. The blue signal shows the surface temperature of the conductor in °C, the green the reference value to Kårehamn in MW.

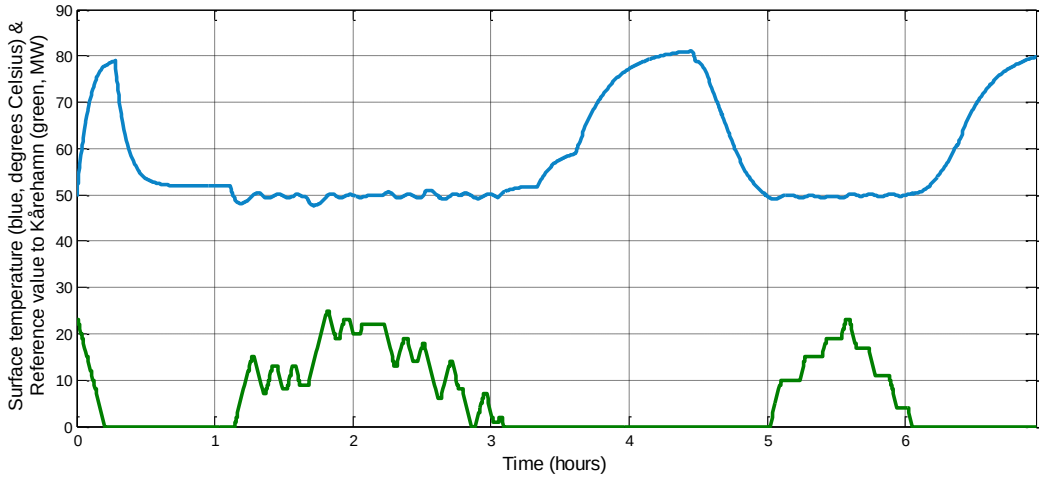

Figure 6-4. Result of simulation, for varying wind speed at conductor, with 0 degrees wind direction and 40 °C ambient temperature. The blue signal shows the surface temperature of the conductor in °C, the green the reference value to Kårehamn in MW.

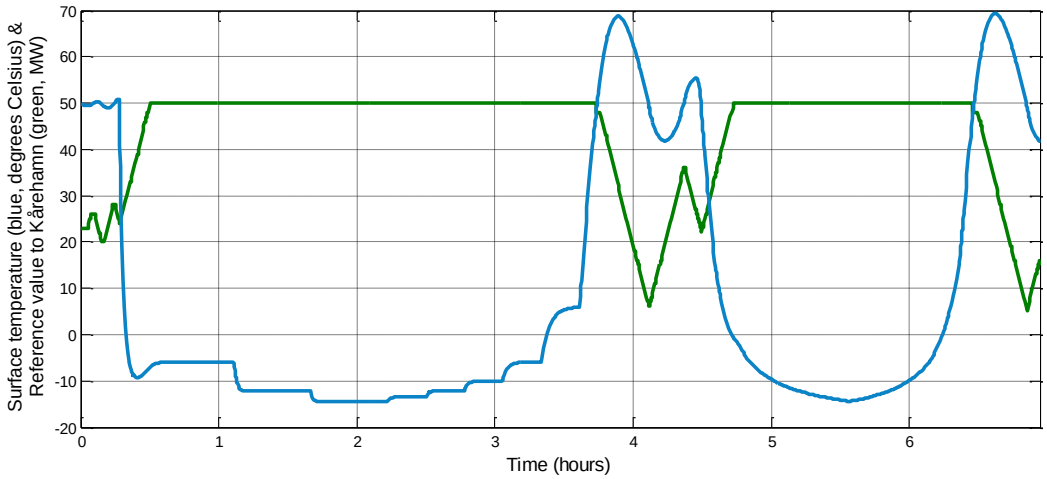

Figure 6-5. Result of simulation, for varying wind speed at conductor, with 90 degrees wind direction and -20 °C ambient temperature. The blue signal shows the surface temperature of the conductor in °C, the green the reference value to Kårehamn in MW.

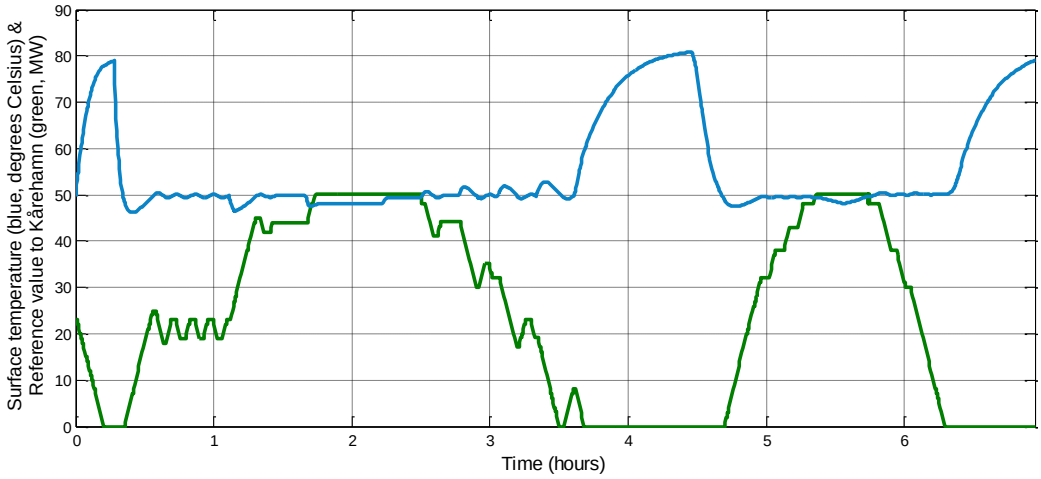

Figure 6-6. Result of simulation, for varying wind speed at conductor, with 90 degrees wind direction and 40 °C ambient temperature. The blue signal shows the surface temperature of the conductor in °C, the green the reference value to Kårehamn in MW.

The look of both the reference signal and surface temperature mimic those made in section 5.2.1, which was expected. There are some major differences however, most notably the large overshoots in Figure 6-3 and Figure 6-5, while in Figure 5-6 and Figure 5-8 there were no overshoots. We can also see quite major changes in the reference value constantly, oscillations even, especially in Figure 6-6. This is partly due to a lack of predictive control.

6.1.2 Changing wind direction in relation to conductor

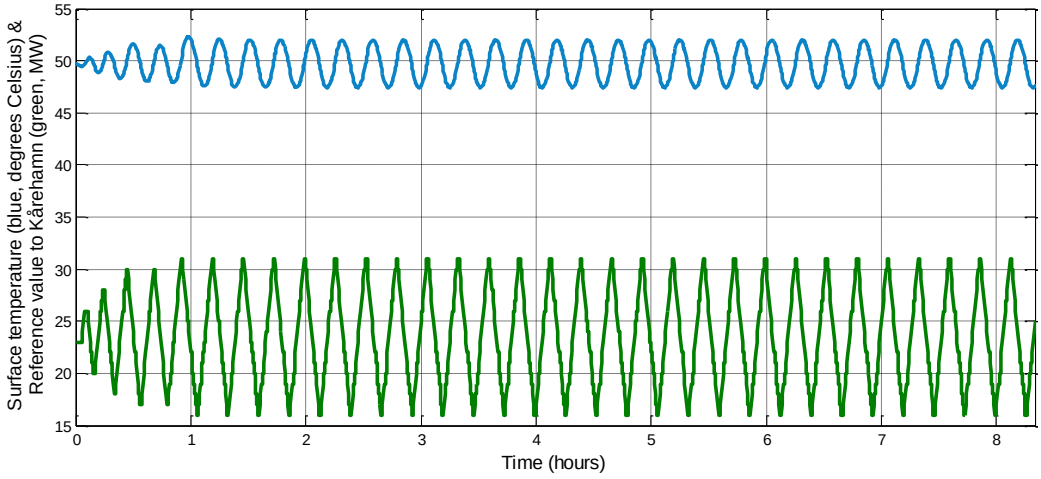

Figure 6-7. Result of simulation, for varying wind direction on conductor, with 0 m/s wind speed and -20 °C ambient temperature. The blue signal shows the surface temperature of the conductor in °C, the green the reference value to Kårehamn in MW.

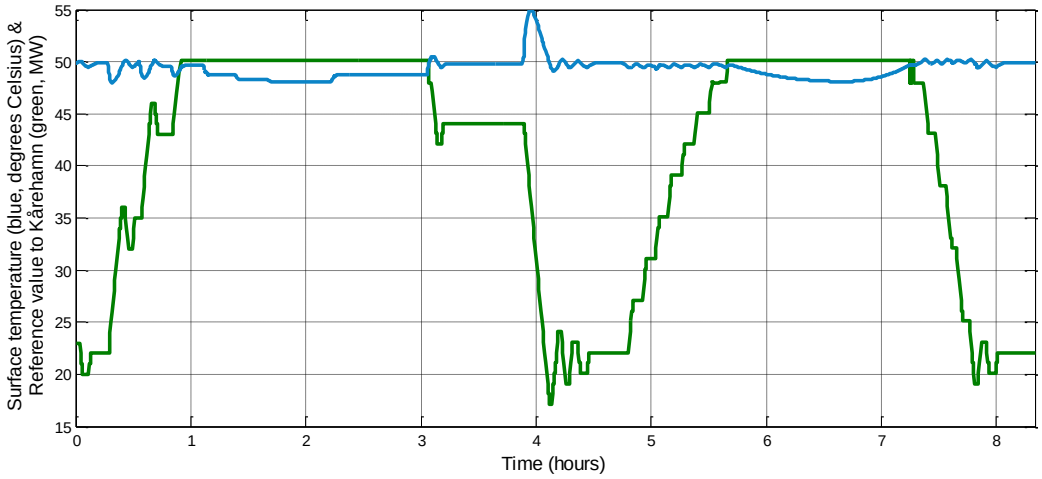

Figure 6-8. Result of simulation, for varying wind direction on conductor, with 15 m/s wind speed and 40 °C ambient temperature. The blue signal shows the surface temperature of the conductor in °C, the green the reference value to Kårehamn in MW.

These simulations also mimic those made in chapter 5 quite well. Though here we clearly see this systems main fault, and it stems from the fact there is no predictive or integral regulation. There are a lot of oscillations, especially in Figure 6-7, which shows steady-state conditions with reference value higher than 0 but lower than maximal output; and where both the reference signal and surface temperature will oscillate without converging. Two simulation cases – no wind and 40 °C, as well as 15 m/s wind speed on the conductor and -20 °C – showed similar results as the simulations in the previous chapter, i.e. steady state values, with 0 MW and maximum output respectively.

6.1.3 Changing ambient temperature at conductor location

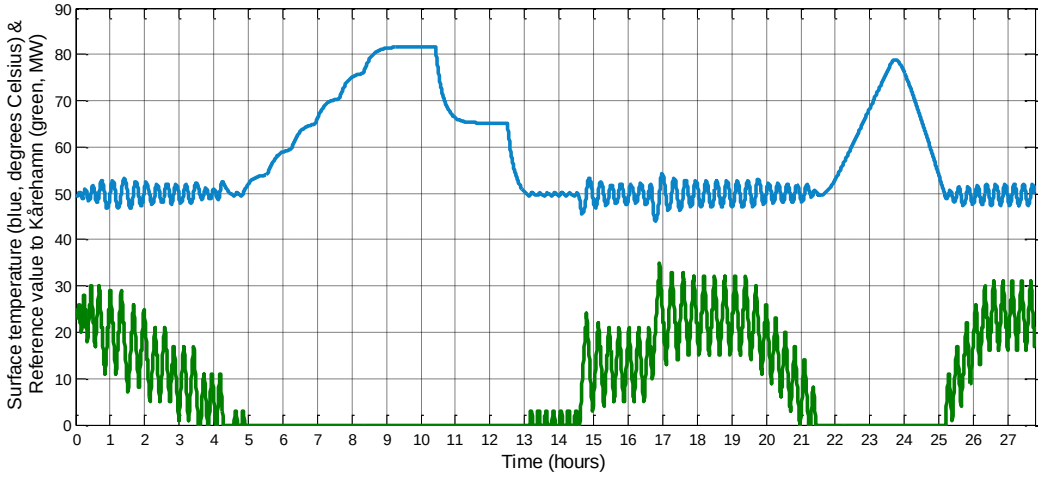

Figure 6-9. Result of simulation, for varying ambient temperature at conductor, with 0 m/s wind speed and varying wind direction. The blue signal shows the surface temperature of the conductor in °C, the green the reference value to Kårehamn in MW.

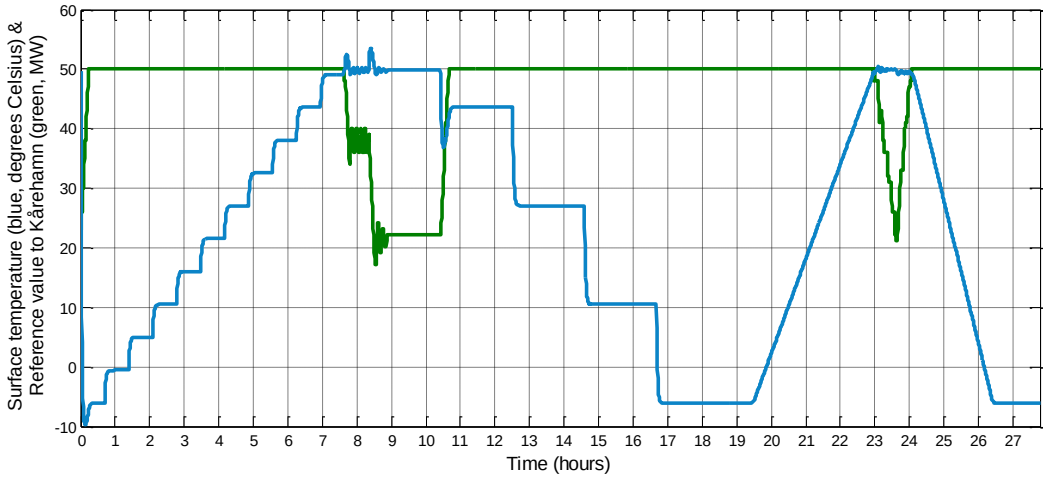

Figure 6-10. Result of simulation, for varying ambient temperature at conductor, with 15 m/s wind speed and 0 degrees direction. The blue signal shows the surface temperature of the conductor in °C, the green the reference value to Kårehamn in MW.

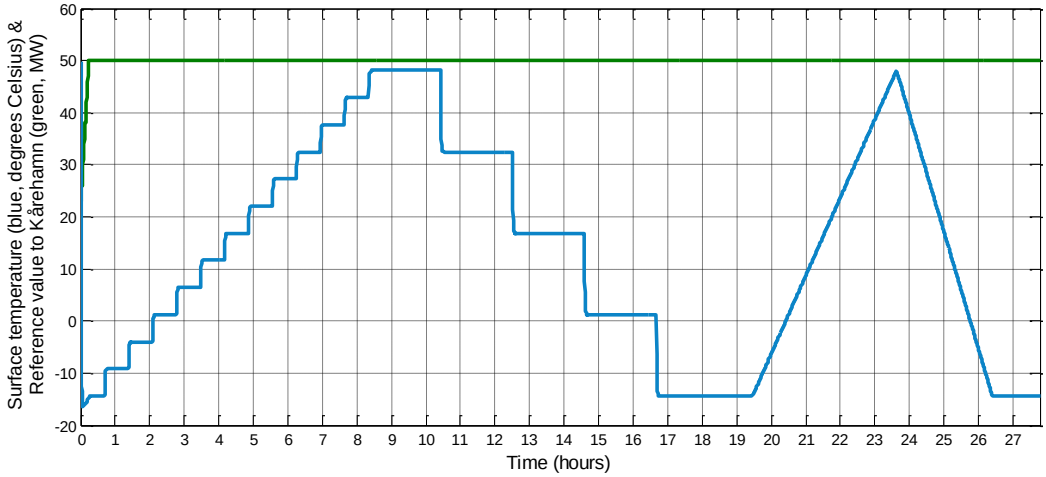

Figure 6-11. Result of simulation, for varying ambient temperature at conductor, with 15 m/s wind speed and 90 degrees direction. The blue signal shows the surface temperature of the conductor in °C, the green the reference value to Kårehamn in MW.

Here it again becomes apparent that this model can't converge, as both signals oscillate. In Figure 6-11 we do see a positive effect of this model however, in that the reference value stays at a constant max, as opposed to Figure 5-15 in section 5.2.3, where the reference value signal had slight dips between six and eight hours in. This is because the surface temperature doesn't exceed 49.5 °C, thus not triggering any control action.

Chapter 7. Secondary aims

As stated in section 1.2, it was also the aim of this thesis to implement error handling in different ways. This included not just errors in the system, but also to find a way to handle the additional generation units, which in this case is a solar power unit and a wind power unit.

Controlling these additional units would be done by sending them a binary signal, telling them if they were allowed to be connected to the grid or not.

The control of the output of Kårehamn by this model will not be needed most of the time, according to E.ON themselves [4] and also seen when looking at the simulation results during this thesis, especially in Figure 4-3 and Figure 4-4 ,which are meant to resemble a normal case. Some of the temperatures are driven up because of the external power and configurations in the model, but they still support that the model would ideally not be used during normal operations.

When the surface temperature of the conductor gets too high however and the model needs to regulate, it is expected to work and reduce the output of the wind turbines. Should it not work – if the turbines don't respond to the signal sent by the model or any other similar error – there must be steps taken so that the surface temperatures of the conductors does not reach critical levels. These include the ability to instead send signals with preset values as reference values if the temperature gets too high but not yet critical; and the ability to send a signal for a hard shut-off signal should the temperature reach critical levels.

7.1 Additional solar and wind power generation units

The power generation sites in question lie north of Föra, and they feed the grid from there. As stated, it is desirable to be able to send a signal, telling them if they can be connected or not. They are private units connected to the grid, and not necessarily delivering power at all times which means their priority as opposed to Kårehamn is lower. This means they should be the first to be disconnected in the case of too high a surface temperature, and subsequently be the last to be connected again. Only when Kårehamn is at unlimited operation and there is room for more power, should they be allowed to be connected to the grid.

To be able to meet that criterion, two parts were added to the model in Figure 5-1. The subsystem block called "Subsystem for handling external power", and several different mathematical operations to calculate the ampacity as well as the ampacity difference. The ampacity calculations are briefly shown and explained in chapter 3. The reason for calculating the difference is the idea that there is a capacity surplus when the surface temperature is below 50 °C yielding a positive ampacity difference, a difference that decreases to 0 when the temperature reaches 50 °C. The most critical line and measurement station thus has the smallest ampacity difference, and it is that number that is being used and that will determine if it is okay to have the additional power connected to the grid.

The subsystem for handling the additional power can be seen below in Figure 7-1:

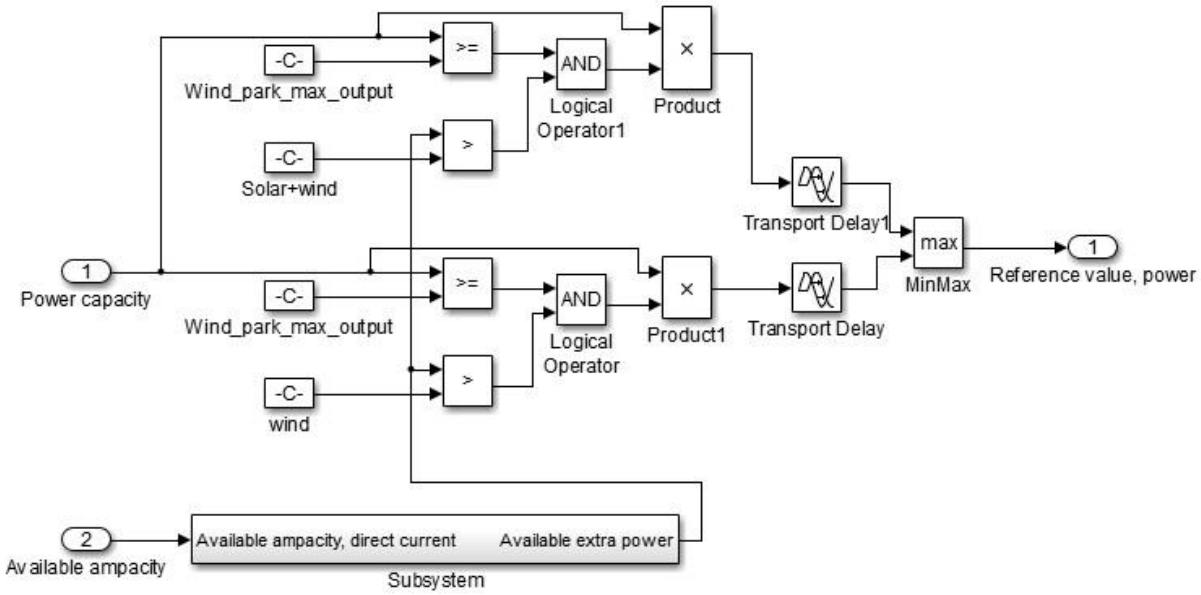

Figure 7-1. Subsystem for handling additional power generating units.

At the left are the two inputs, “Power capacity” and “Available ampacity”. They are basically the available capacity at current surface temperature, and the available ampacity, essentially the available power capacity excluding Kårehamn. The power capacity is compared with the maximum available output from Kårehamn to check that it’s greater. Meanwhile, the ampacity – after conversion operations - is compare to check that it’s greater than the maximum available output from the additional generation units. Only if these two comparisons are both true, the additional generation units are permitted to connect to the grid. They are both checked to make sure the right value is outputted. There is also a delay, which had to be installed to make the system function without errors when the additional units would connect and disconnect instantly and constantly.

7.2 Giving Kårehamn preset output value

If the surface temperature of the conductors gets too high, but not yet critical, and it doesn’t react to changes in the reference value to Kårehamn, something must be done. When the temperature reaches a pre-defined value that is too high and exceeds it for a period of time without reaching critical values, preset values for the power delivered by Kårehamn that are known to work, should be used. In this model, 60 °C is used, but this value can be defined. A model for checking and handling this can be seen below.

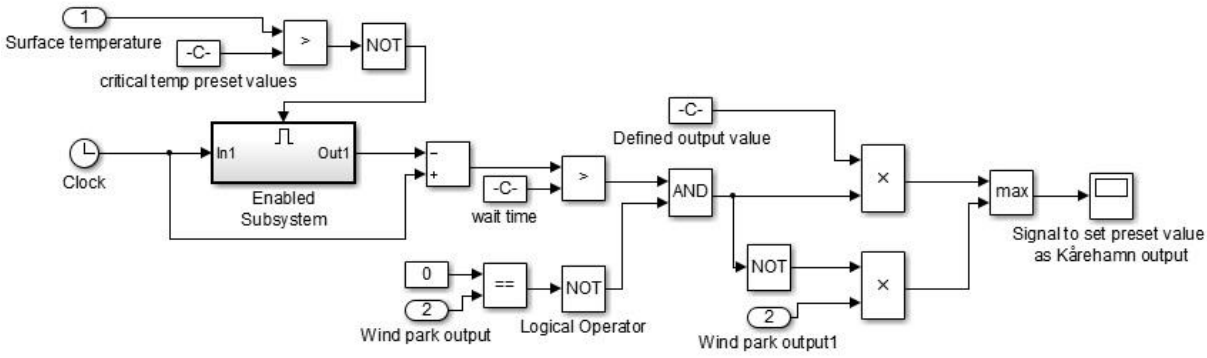

Figure 7-2. Subsystem for handling too high surface temperatures, where the Kårehamn output needs to be set according to a safe, preset value.

Seen in Figure 7-2 is the content of the subsystem called “Method for handling too high, yet not critical temperatures” in Figure 5-1. There are two inputs, the surface temperature and the wind farm output. The actual surface temperature is compared to the defined “too high a temperature”, and if it is higher, triggers the enabled subsystem, which starts a counter. That count is then compared to a defined wait time, which was set to 15 minutes. If that relational operator outputs true as a value, which it does after the wait time, and additionally the wind farm is not already shut off, a preset value is sent out as new reference value.

7.3 Kårehamn emergency shutdown

If the surface temperature of the conductors gets too high still, exceeds a critical temperature, and doesn’t cool down after a defined time period, the whole farm must be shut off. The critical temperature used here is 70 °C, with a 5 minutes delay. A subsystem that does this can be seen in Figure 5-1, labeled “Method for shutting down Kårehamn”. A detailed figure of the subsystem can be seen below.

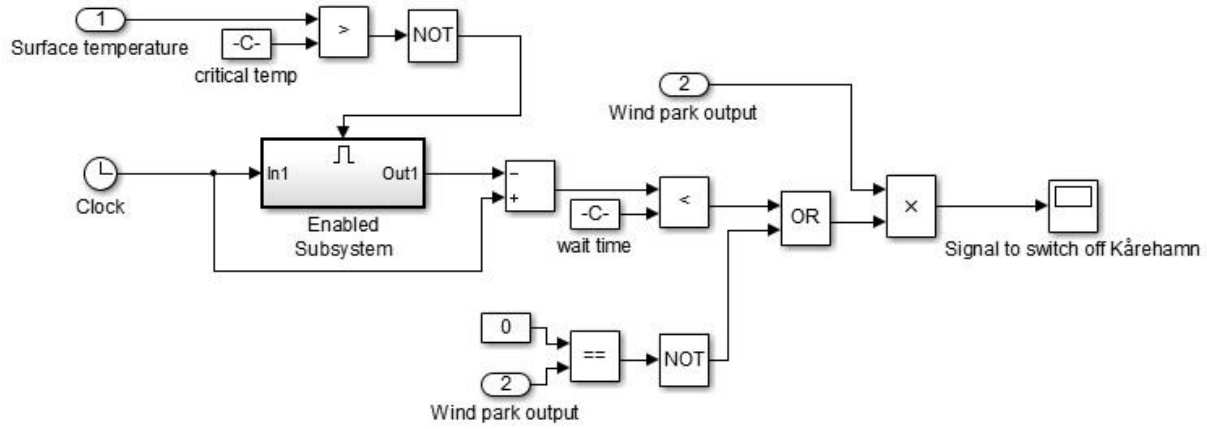

Figure 7-3. Subsystem for handling critically high surface temperatures, where Kårehamn needs to be shut off.

The content of the subsystem is quite similar to that in Figure 7-2 in that it compares the surface temperature to a defined value, which starts a counter, which in turn is compared to a defined wait time. When that is true, and the wind farm output is checked to see that it is not already shut off, the logic operator outputs a 0 which shuts off Kårehamn.

7.4 Commissioning – Kårehamn

The wind farm is expected to be commissioned in late 2013. The wind turbines themselves will be installed during a period of time, so it desirable to be able to test the model built in this thesis on only one wind turbine initially to determine its effectiveness and that it works.

Since the model is built around the complete farm with an output of 48 MW though, adjustments would have to be made. An easy way of implementing this, given the time constraints and the fact that this was not the primary goal of the thesis, would be to simply adjust the power to and from Kårehamn. Upon completion, Kårehamn will comprise of 16 separate 3 MW wind turbines, which means the power values could simply be adjusted a factor 16 so that the system could be tested on one wind turbine initially. This would also mean the current - converted from the wind farm power output – through the line, had to be scaled up in the control model, so the regulator would function correctly, since only adjusting the power output by a factor 16, would not affect the thermal model in a way that the surface temperature would reach high enough values.

Chapter 8. Conclusions

This thesis aimed at constructing a Simulink model which incorporated a thermal model – for measuring the surface temperature of the conductors on Öland – and regulator in order to control the power output from E.ON's new offshore wind farm, Kårehamn. The complete model built is shown in Figure 5-1, and was constantly successful in controlling the surface temperature of the most critical of the lines, by controlling the output from Kårehamn.

Before ever building the model, two things were contemplated. Should solar irradiation be included in the model, and which standard for calculating the surface temperature in overhead lines should be used. These things were mentioned briefly in section 2.2 and 4.3. It was decided to include solar irradiation. Mostly to safeguard the model, but also because the CIGRE 207 standard included a simplified equation for the solar gain, with parameters easily found and incorporated. The question of which standard to use was not so straight forward, but the CIGRE 207 standard was chosen. Mostly because the report [5] used it and that was the report first found on the subject, but also because [3] used both, with discussions clearly stating very small differences between the two, most of the time.

After building the thermal model, but before building the larger model and incorporating control, it was verified to ensure it functioned satisfactory. The CIGRE report included several tests of its equations, so it was natural to test them with the model used in this thesis and compare the results. They were similar for the most part. There were, however, instances in the last two tests where the results differed, sometimes significantly (see sections 4.1.3 and 4.1.4). What caused these differences never became known, but it was still decided to move forward, because the model behaved correctly in terms of how the surface temperature changed and because everything except the times involved were very similar. It was also thought that these max and min temperature values were more important for the function of the model, rather than the time. There was also the fact that the comparison was much more similar when calculated numerically, as stated in more detail in section 4.1.5.

While the model was successful in terms of its performance and in controlling the temperature, there is some cause for discussion. First, because external loads and power generating units were incorporated in the model, they tended to skew the simulations and surface temperatures. Generally, because the loads were chosen at their minimum with almost 0 MW at all line sections, and the power generating units chosen as always at maximum output, the surface temperatures were greatly driven up, showing higher temperatures than would be if they were chosen differently or not incorporated at all. The effect of this is clearly shown in Figure 5-7, Figure 5-9 etc., where the surface temperature settles at about 80 °C as its maximal value, even with Kårehamn totally shut off. That value could be higher still would the simulations be made on line sections in Högsrum or Linsänkan, were the external power inputs would be even more. Second, the parameters chosen for the PID regulator as its configuration, greatly affected the results. They were chosen - as explained in section 5.1 - based on a worst case scenario, though it is very plausible a different set of parameter configuration could have provided a better control, would a different set of tools and more extensive knowledge in choosing those parameters be available.

In the model, it was initially thought of to have delays installed throughout but mainly after the controller, to mimic the real case. In the real case, there surely exist such a delay between a signal

sent from the model, to an actual, physical change in the wind turbines output. Such delays were not included in the model however, as the placement and magnitude of the delays could not be easily decided. It is worth mentioning here though.

During the building and testing of the alternative incremental control design in chapter 6, there were no real surprises. The model functioned correctly, and controlled the surface temperature based on the Kårehamn output. There were however, several concerns. The biggest concern was the fact that it was oscillating at steady-state temperature, which would certainly cause stress on the wind turbines as the reference signal varied as wildly as up to 15-20 MW in some cases, albeit with relatively small temperature variations. The second concern was the parameters in the integrator, or more generally, the wait time between output changes, and the size of the output changes. These parameters directly affected the model's performance, and also the severity of the oscillations. Default values were 30 seconds and 1 MW respectively. Higher output change and/or lower wait time would make the control faster with generally smaller overshoots, but would cause more severe oscillations in the reference output value. Lower output change and/or higher wait time on the other hand, would make the control slower with more severe overshoots, but would limit the degree of oscillations, sometimes even eliminating them.

When comparing the two control algorithms, that of this thesis' and that of the alternative incremental one, it was clear the one constructed here is better. Its main drawbacks are described above, and the simulations clearly confirm that the controller constructed here is superior. This is evident when viewing the simulations made for the two methods. Looking at Figure 6-7 or comparing Figure 5-13 and Figure 6-9, it can be seen that the alternative control method oscillates greatly. And when comparing Figure 5-6 and Figure 6-3 for example, the lack of predictive regulations mean the alternative control creates major overshoots that are almost non-existent in the model used in this thesis.

Lastly, there was some cause for concern about the two additional power generating units discussed in section 7.1. As stated, this model simply checked if Kårehamn was at its maximum output and if there was enough available ampacity. There were no real smart system, and in several cases, they would be connected to the model, only to drive up the surface temperature to the degree they would have to be immediately disconnected, after which they were connected again, and so on. A model with some sort of predictive element or some sort of wait time after being connected or disconnected would possibly solve this problem.

Chapter 9. Continued Work

While this model is very much complete and functional in the task defined for it, there is room for improvement in some aspects. These mainly regard the PID controller and the method for handling the additional generation units on the grid.

As discussed briefly in the conclusion, there is almost certainly a better configuration for the parameters in the PID controller, and if one were to have better tools or more extensive knowledge, it could surely be improved upon.

Regarding the additional wind and solar power; the main problem is the lack of any predictive element, which (as discussed in the conclusion) would cause these power generating units to be connected and immediately disconnected, only to immediately be connected again, until changes in external parameters changed the surface temperature in either direction. A delay of some sort could possibly be installed, to partly solve this problem.

It would have been desirable to implement some sort of method for verifying the incoming data, the weather parameters as well as the current and surface temperature measured at the three line sections; however there was no time to develop such a method. The weather parameters could possibly be compared to nearby weather stations if such exist. One could also compare the values for the data received at both Linsänkan and Högsrum, because they lie very close to each other geographically, their measured data should be very similar. This would definitely be ground for further work.

References

[1]. B. Lundkvist et al., ”Energiläget 2012”, Energimyndigheten, Eskilstuna, Oct. 2012.

[2]. Stadsrådsberedningen. (2005, March 16). *Europa 2020 – EU:s gemensamma tillväxt- och sysselsättningsstrategi* [Online]. Available: http://www.regeringen.se/sb/d/2504

[3]. AREVA, “MiCOM P341, Dynamic Line Rating Protection Relay”, Application Guide, AREVA, 2010.

[4]. C. Ahlrot, E.ON, private communication, January 2013.

[5]. Working Group 22.12, “Thermal behaviour of overhead conductors”, Technical brochure #207, CIGRE, 2002.

[6]. IEEE Power Engineering Society, “IEEE Standard for Calculating the Current-Temperature of Bare Overhead Conductors”, Standard 738, IEEE, Jan. 2013.

[7]. British Standards, “Electric cables – Calculations of the current rating”, IEC 60287, British Standards, July 2002.

[8]. European Commission Joint Research Centre, Institute for Energy and Transport. *PV potential estimation utility* [Online]. Available: http://re.jrc.ec.europa.eu/pvgis/apps4/pvest.php

[9]. The Engineering Toolbox. *Surface Absorptivities* [Online]. Available: http://www.engineeringtoolbox.com/radiation-surface-absorptivitie-d_1805.html

[10]. The Engineering Toolbox. *Emissivity Coefficients of some common Materials* [Online]. Available: http://www.engineeringtoolbox.com/emissivity-coefficients-d_447.html

[11]. C. Ahlrot, private communication, February 2013.

[12]. Google. (2010). *Google höjdkarta* [Online]. Available: http://www.sk6lk.se/elev_path.html

[13]. C. Ahlrot, E.ON, private communication, February 2013.

[14]. C. Ahlrot, E.ON, private communication, May 2013.

[15]. KHCK. *BARE CONDUCTOR AND WIRES* [online]. Available: http://www.khck.hk/Catalog/ENERGY&POWER-PRODUCT/Power-Equipment/bare-conductor-and-wires.pdf

Appendix A, Cable data

Cable type 157 Al59:

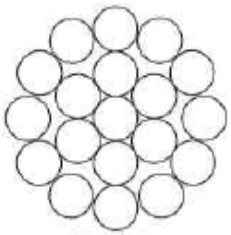

19 trådar

(1+6+12)

R_{dc}= 0,186 ohm/km
R_{ac}= 0,205 ohm/km (50°C)
D= 16,3 mm
α= 3,8 *10^{-3} 1/K
β= 4,5*10^{-4} 1/K
m = 437 kg/km
c= 960 J/(kg*K)

Cable type 329 Al59:

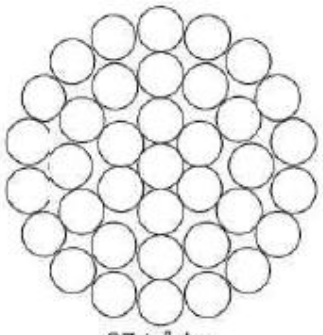

37 trådar

(1+6+12+18)

R_{dc}: 0,0899 ohm/km
R_{ac}: 0,0993 ohm/km (50°C)
D: 23,6 mm
α=3,8 *10^{-3} 1/K
β= 4,5*10^{-4} 1/K
m =910 kg/km
c=960 J/(kg*K)

Appendix B, Simulink model m-file

```
% File for initiating values in the Complete Model
% --Values relating to Kårehamn and model
T_initial = 49.75;                      % Initial guess for the surface
temperature of the conductor (degrees Celsius)
Wind_park_max_output = 48;              % Maximum output from Kårehamn (MW)
Critical_temperature_presetvalues = 60; % Maximum allowed surface
temperature before preset values are used (degrees Celsius)
Wait_time_critical_temperature = 900;   % Time to wait with surface
temperature above critical before preset values are used (seconds)
Preset_output_value = 25;               % Preset output value incase too
high temperature (MW)
Critical_temperature_shutoff = 70;      % Maximum allowed surface
temperature before shut off is required(degrees Celsius)
Wait_time_critical_shutoff = 300;       % Time to wait before Kårehamn is
shut off (seconds)
% --Miscellaneous values
Irradiation_glb = 560;                  % Global irradiation (W/m2)
height = 42;                            % Height above sea level (m)
gravity_g = 9.82;                       % Gravity of earth (m/s2)

% --Location specific values
wind_dir = 0; % Enter winddirection (0-359 degrees)
                % 0 degrees equals winds blowing south, 90 degrees winds
                % blowing east, 180 degrees winds blowing north and 270
degrees
                % winds blowing west.
                % OBS! Kolla upp faktisk ledningsriktning!
if wind_dir >= 0 && wind_dir <= 67.5
    dir_Kpg = 90 - wind_dir;
    dir_Hrm = wind_dir + 22.5;
    dir_Lin = wind_dir + 22.5;
elseif wind_dir > 67.5 && wind_dir <= 90
    dir_Kpg = 90 - wind_dir;
    dir_Hrm = 157.5 - wind_dir;
    dir_Lin = 157.5 - wind_dir;
elseif wind_dir > 90 && wind_dir <= 157.5
    dir_Kpg = wind_dir - 90;
    dir_Hrm = 157.5 - wind_dir;
    dir_Lin = 157.5 - wind_dir;
elseif wind_dir > 157.5 && wind_dir <= 180
    dir_Kpg = wind_dir - 90;
    dir_Hrm = wind_dir - 157.5;
    dir_Lin = wind_dir - 157.5;
elseif  wind_dir > 180 && wind_dir <= 247.5
    dir_Kpg = 270 - wind_dir;
    dir_Hrm = wind_dir - 157.5;
    dir_Lin = wind_dir - 157.5;
elseif wind_dir > 247.5 && wind_dir <= 270
    dir_Kpg = 270 - wind_dir;
    dir_Hrm = 337.5 - wind_dir;
    dir_Lin = 337.5 - wind_dir;
elseif wind_dir > 270 && wind_dir <= 337.5
    dir_Kpg = wind_dir - 270;
    dir_Hrm = 337.5 - wind_dir;
    dir_Lin = 337.5 - wind_dir;
elseif wind_dir > 337.5 && wind_dir <= 359
    dir_Kpg = wind_dir - 270;
    dir_Hrm = wind_dir - 337.5;
    dir_Lin = wind_dir - 337.5;
end
```

```
% --Köping
Ta_Kpg = -20;     % Ambient temperature (degrees Celsius)
V_Kpg = 15;       % Wind velocity (m/s)
% --Högrum
Ta_Hrm = -50;     % Ambient temperature (degrees Celsius)
V_Hrm = 20;       % Wind velocity (m/s)
% --Linsänkan
Ta_Lin = -50;     % Ambient temperature (degrees Celsius)
V_Lin = 20;       % Wind velocity (m/s)

% --Cable specific values
D_cable157 = 16.3*10^-3;                % Total diameter, cable 157 al59
(m)
D_cable329 = 23.6*10^-3;                % Total diameter, cable 329 al59
(m)
d_cable = 3.26*10^-3;                   % Diameter of outer wire (m)
m_cable157 = 0.437;                     % Mass per unit length, cable 157
al59 (kg/m)
m_cable329 = 0.91;                      % Mass per unit length, cable 329
al59 (kg/m)
dc_resistance_cable157 = 186*10^-6;     % Dc resistance per unit length,
cable 157 al59 (kg/m)
dc_resistance_cable329 = 89.9*10^-6;    % Dc resistance per unit length,
cable 329 al59 (kg/m)
ac_resistance_cable157 = 205*10^-6;     % Ac resistance per unit length,
cable 157 al59 (kg/m)
ac_resistance_cable329 = 99.3*10^-6;    % Ac resistance per unit length,
cable 329 al59 (kg/m)
sp_heat = 960;                          % Specific heat capacity (J/(kg*K))
alpha = 3.8*10^-3;                      % Temperature coefficient of
resistance (1/K)
Absorb_al = 0.5;                        % Absorptivity for aluminum
(unitless)
Emiss_al = 0.07;                        % Emissivity for aluminum
(unitless)

% --Grid specific values
% --Loads (given in MW)
Load_fora = 0;
Load_djupvik = 0.000275;
Load_sid = 0;
Load_kpg_line1 = 0.762902;
Load_kpg_line2 = 0.002091;
Load_bhm = 0.000755;
Load_hrm = 0.001647;
% --Wind power on grid (given in MW)
Wind_ltp = 3;       % default vale = 3
Wind_sid = 16;      % default vale = 16
Wind_kpg = 0;       % default vale = 0
Wind_kpg_20 = 20;   % default vale = 20
Wind_bhm = 7.7;     % default vale = 7.7
Wind_hrm = 20;      % default vale = 20
% --External controllable power sources (given in MW)
Solar_expendable = 1.3;
Wind_expendable = 0.8;
```